In-situ opportunities for Bragg Coherent Diffraction Imaging of Materials

Ian Robinson
Ana Estandarte
Ross Harder
Felix Hofmann
Xiao Chen
Yue Cao
Tadesse Assefa
I-16 Diamond
I-07 Diamond
CSX NSLS-II
34-ID-C APS

Condensed Matter Physics and Materials Science Department
Brookhaven National Lab
London Centre for Nanotechnology

Workshop "Energie et Developpement Durable"
Soleil Synchrotron,
March 2018

Outline

- Nanocrystal structures
- Bragg Coherent X-ray diffraction
- Dislocations during crystal growth
- Phase Domain Structures
- Nanoscale alloying
- Focussed Ion Beam Milling
- Cryogenic Sample Examples

Phase Diagram of Gold vs Size

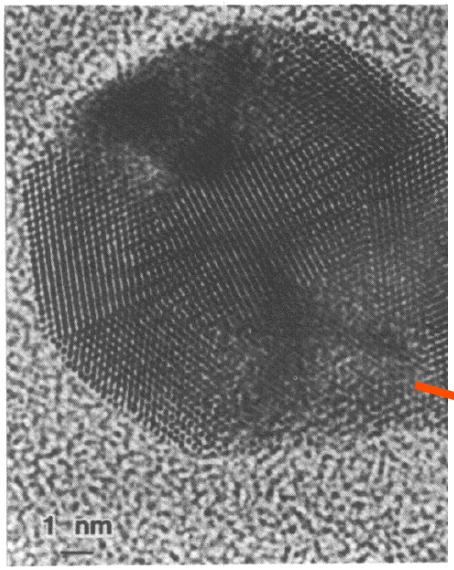

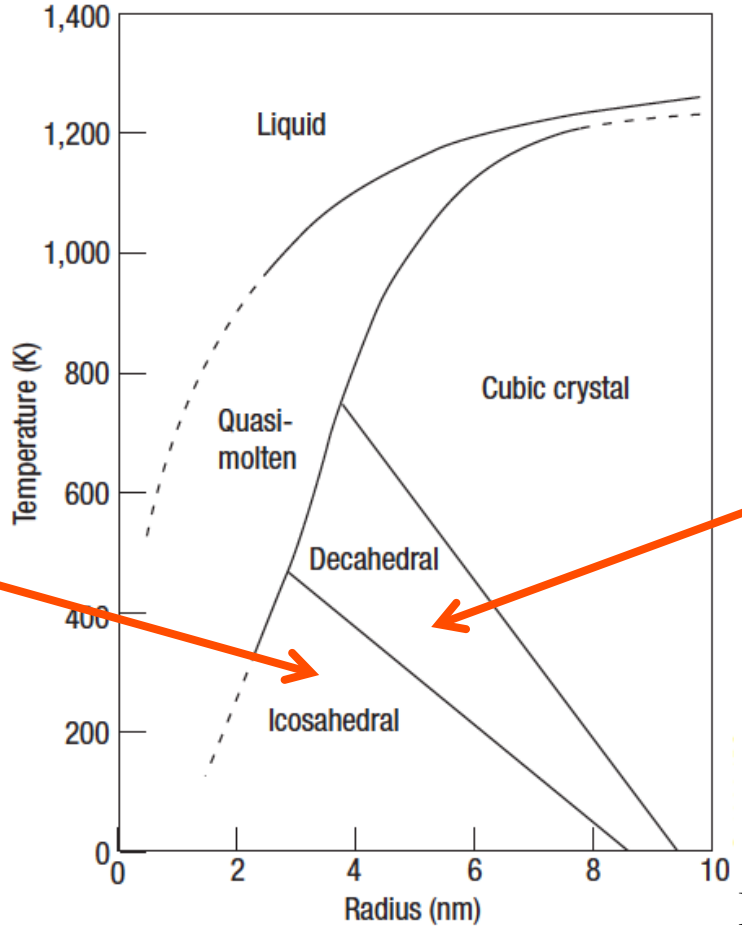

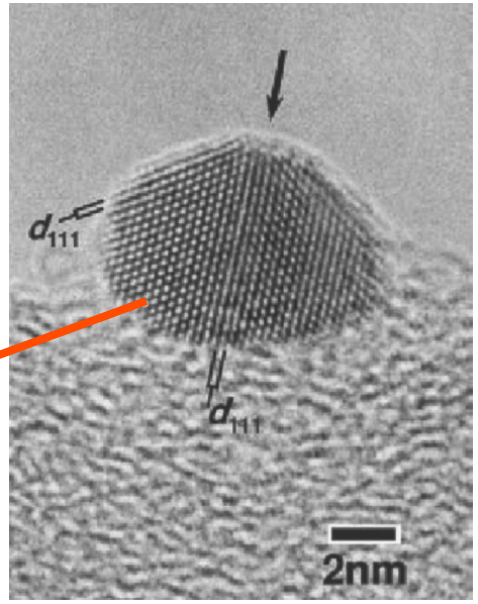

L. D. Marks, RPP (1994)

Koga and Sugawara (2003)

Bragg Coherent Diffraction Imaging "Lensless" X-ray Microscope, 2003

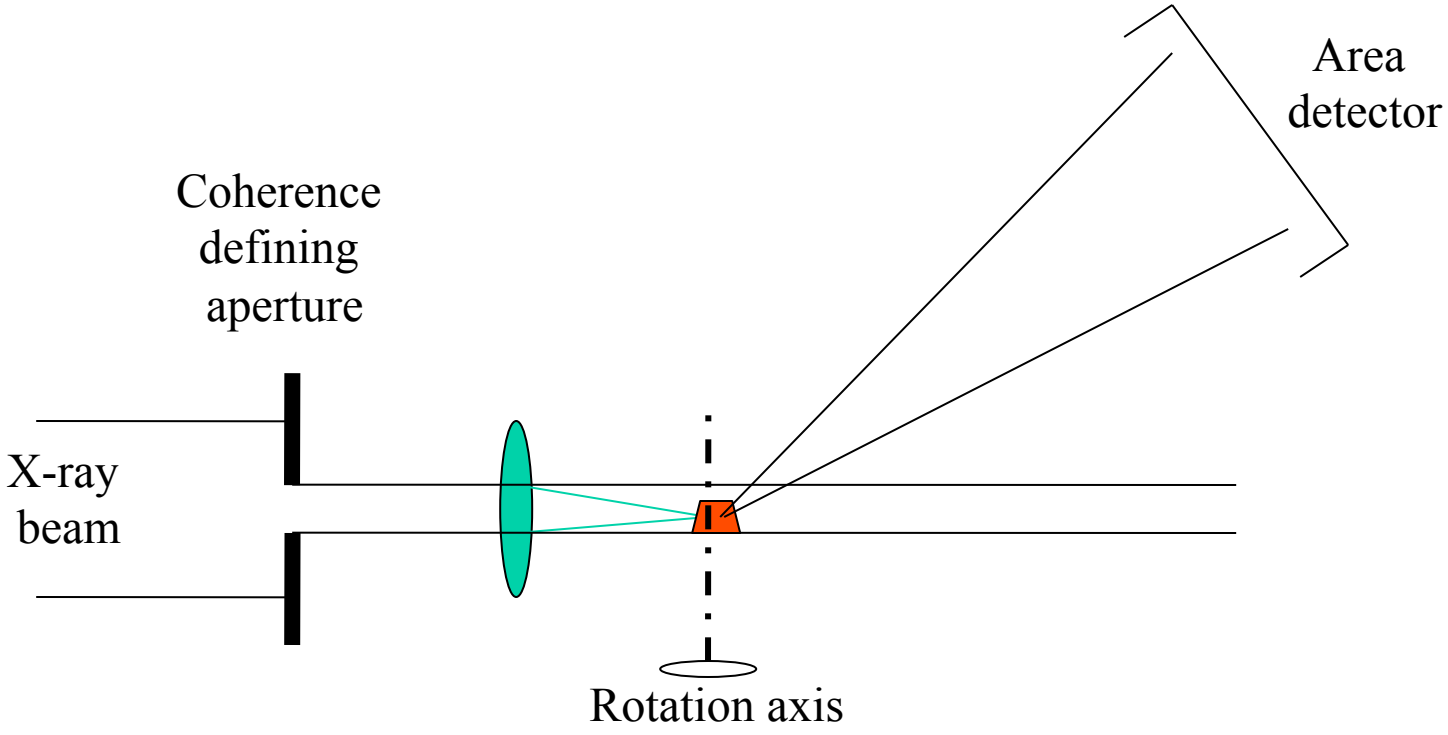

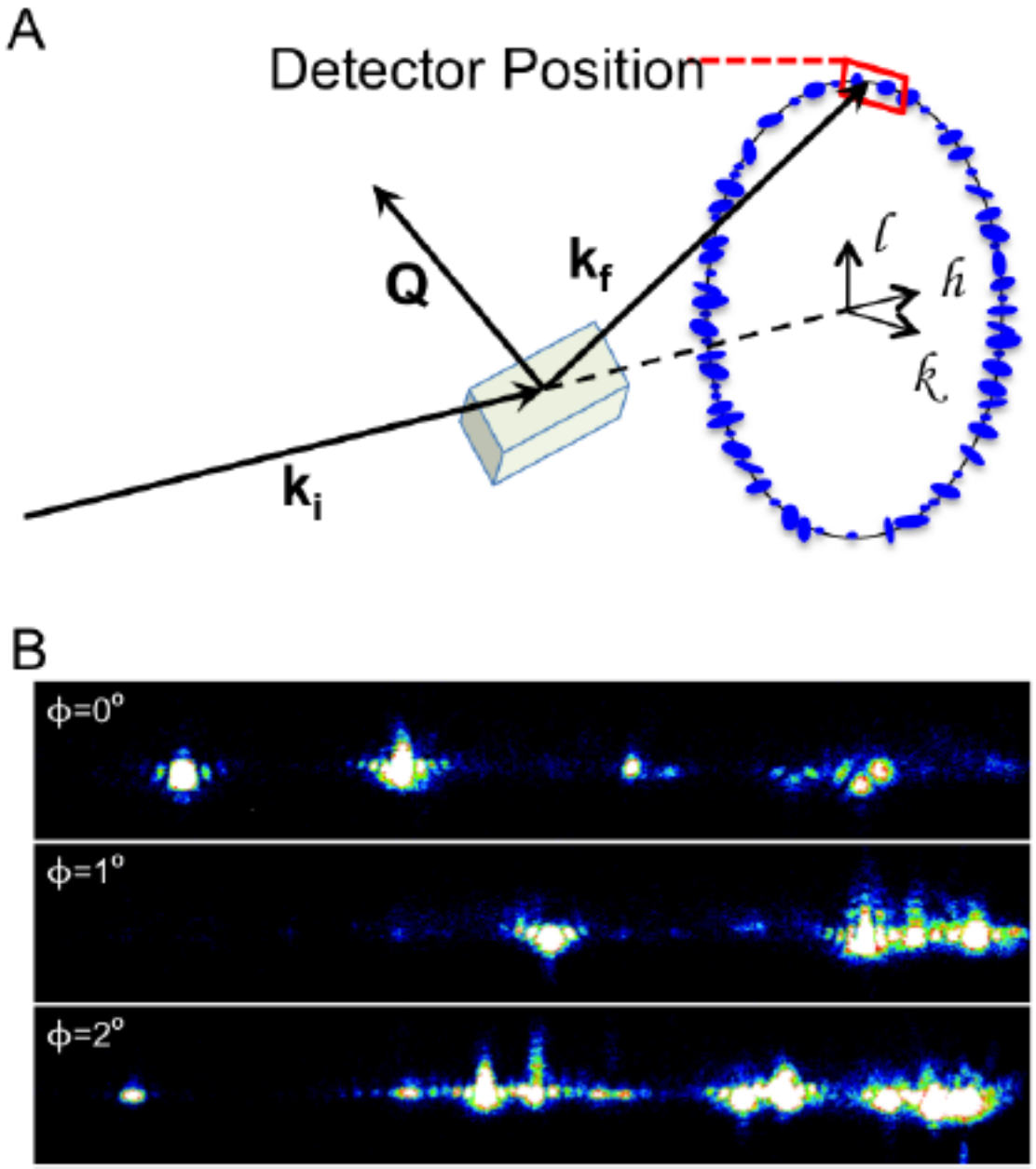
A
Detector Position
Q
k_f
k_i
l
h
k
B
ϕ=0°
ϕ=1°
ϕ=2°

Generic "Error Reduction" method

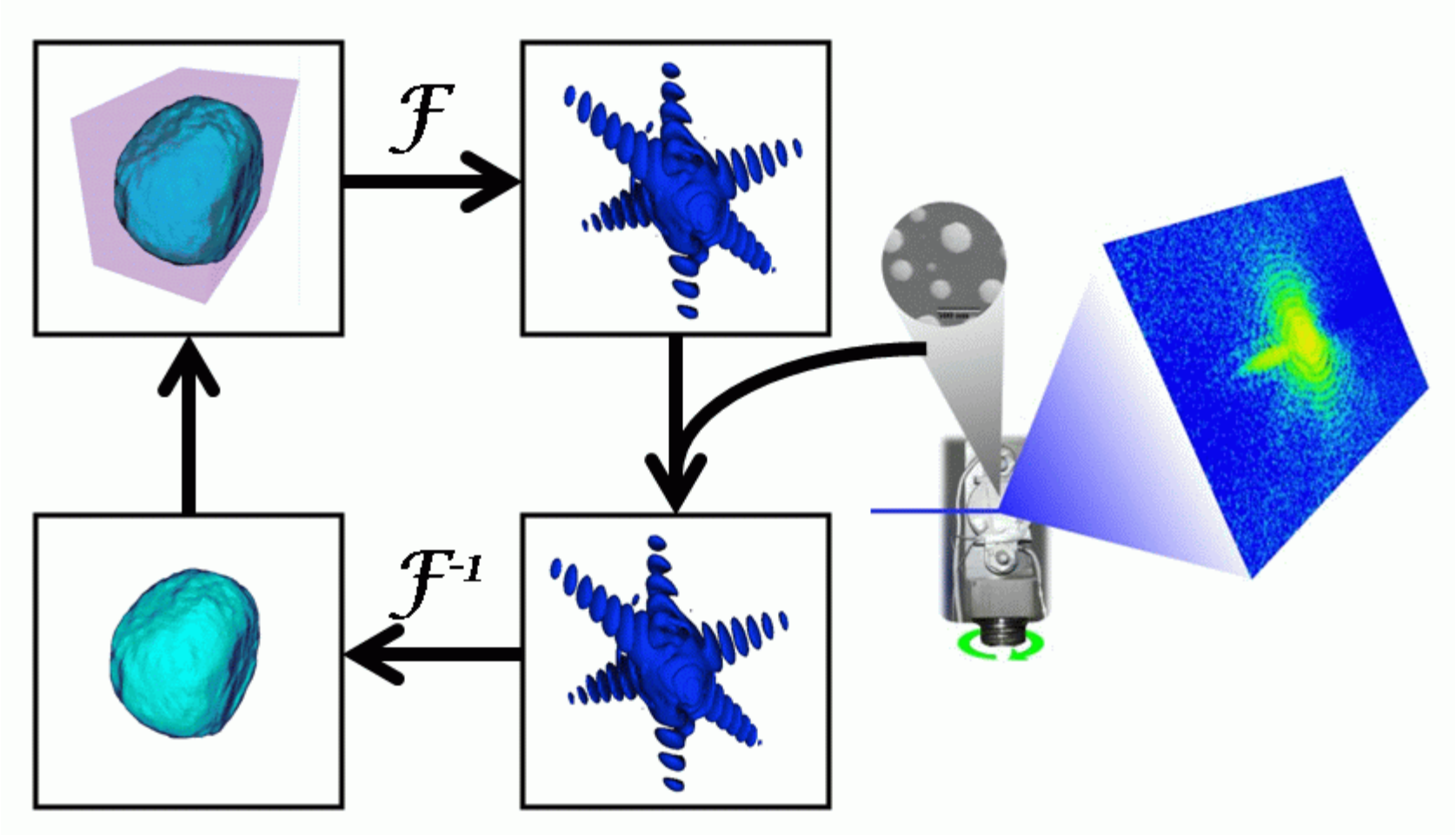

J. R. Fienup Appl. Opt. 21 2758 (1982)
R. W. Gerchberg and W. O. Saxton Optik 35 237 (1972)

Gold nanocrystal reconstruction

showing support used for 20 HIO followed by 10 ER

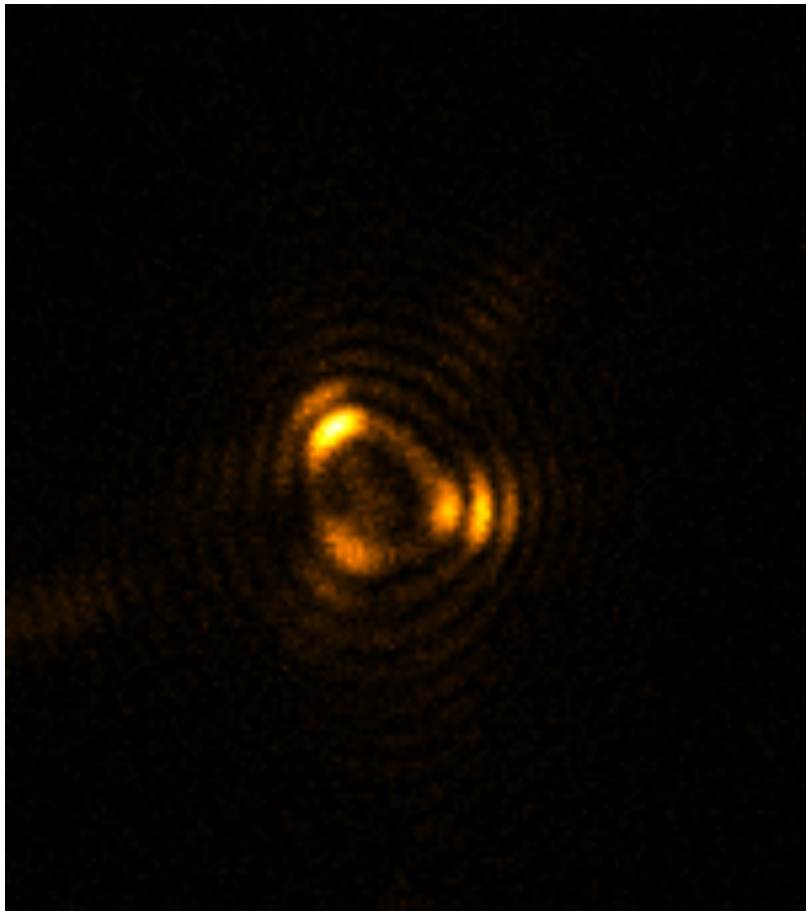

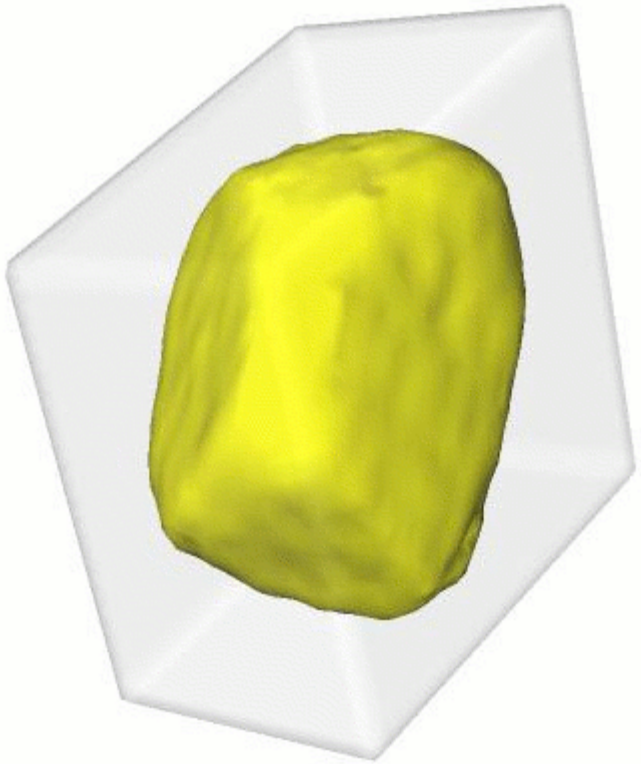

Phase isosurface of residual strain

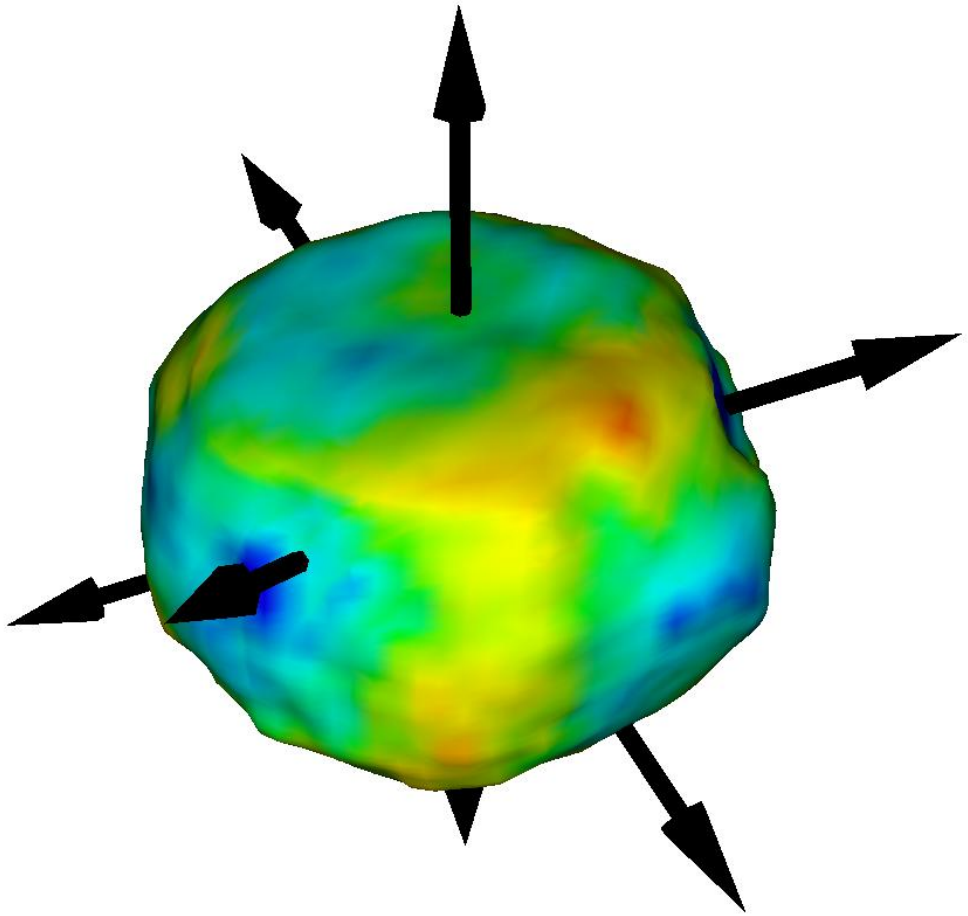

Sensitivity to strain

$$\Delta\varphi = \mathbf{k}_f \cdot \mathbf{u} - \mathbf{k}_i \cdot \mathbf{u} = \mathbf{Q} \cdot \mathbf{u}$$

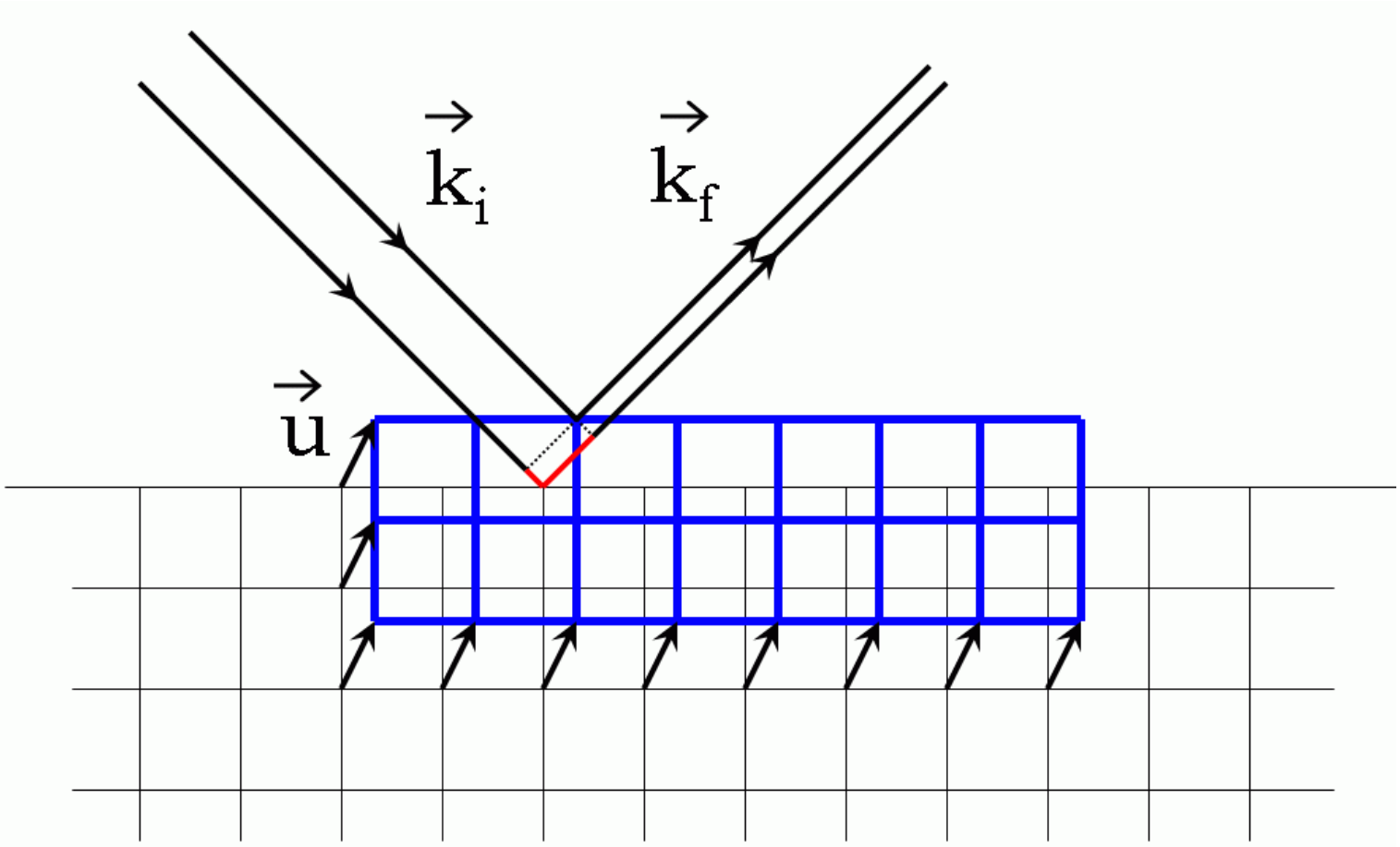

Strain field of Edge Dislocation Loop

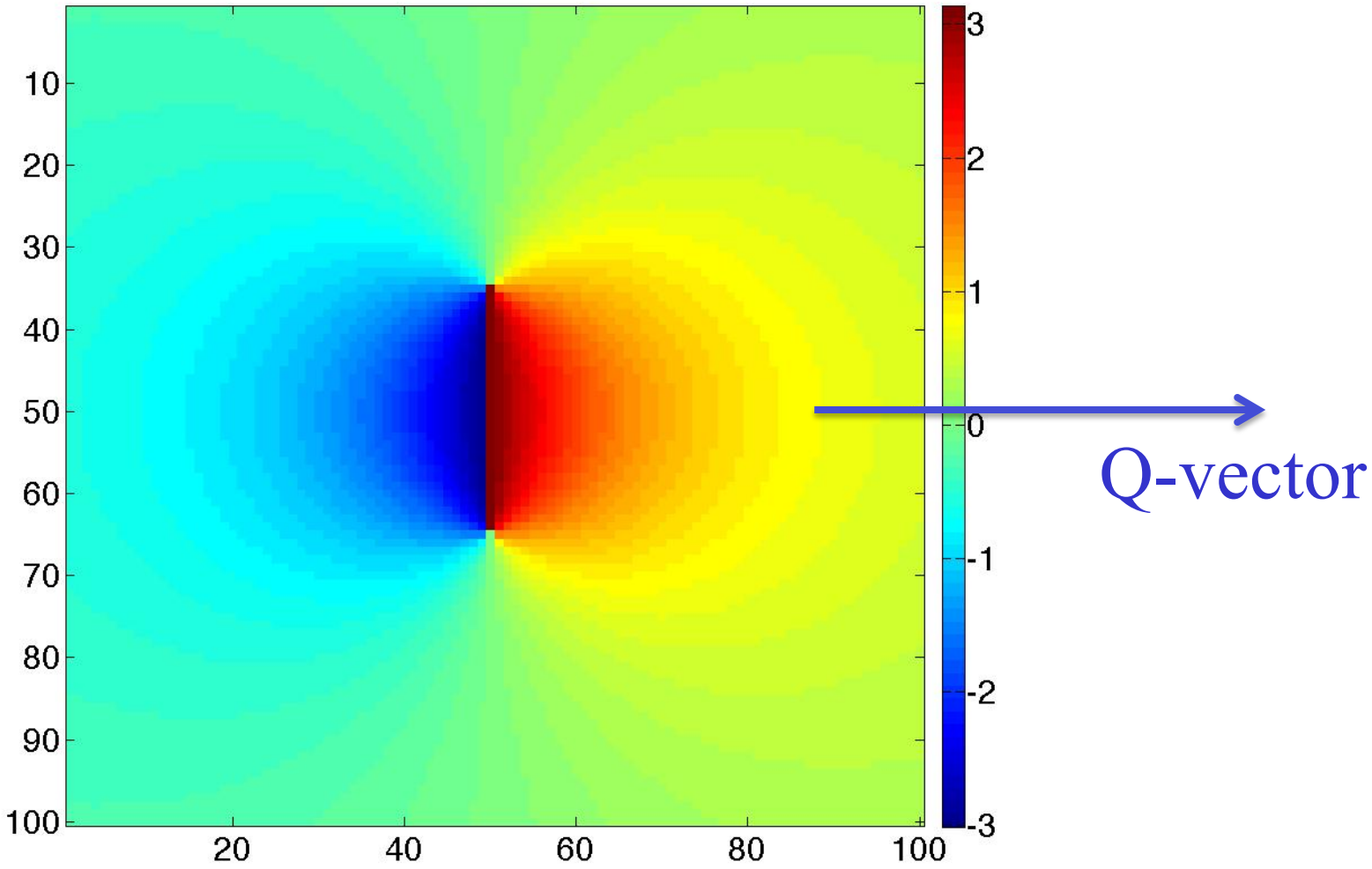

Au NC before Fe deposition

Ana Estandarte, to be published

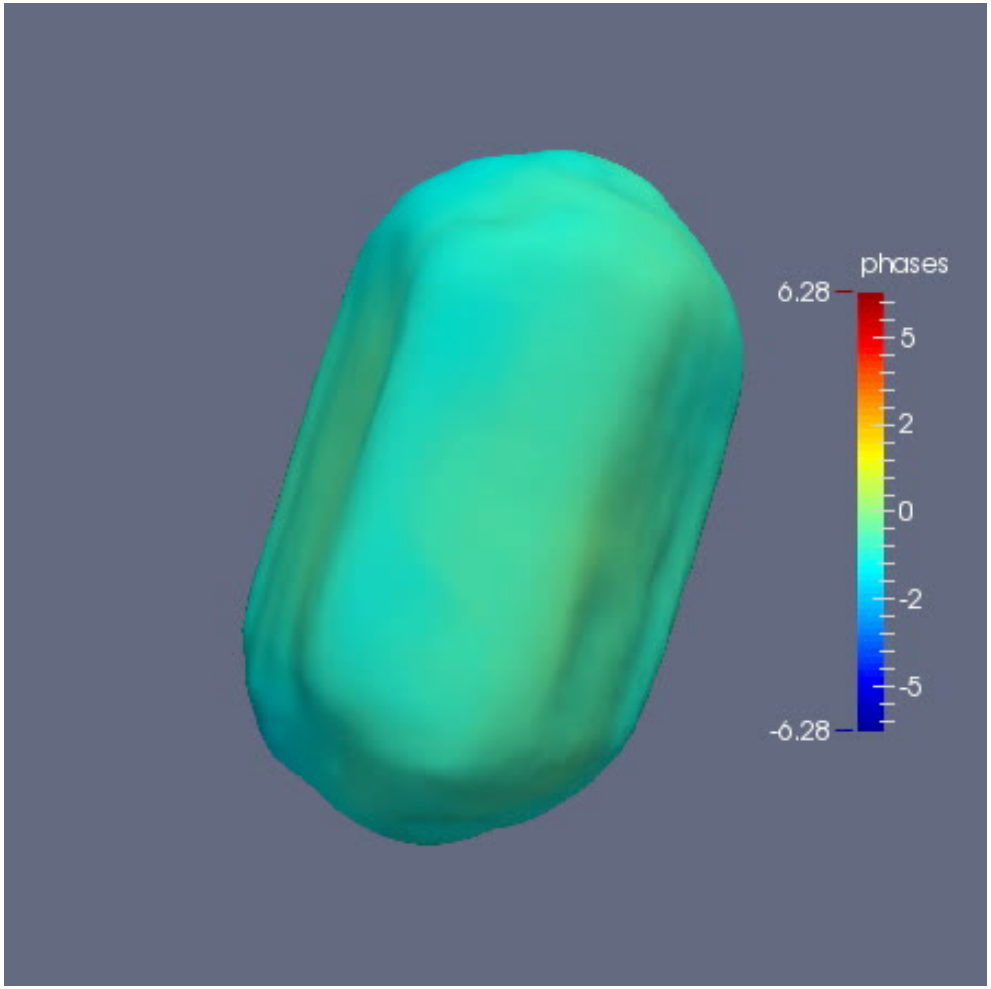

Before dosing

After first Fe dose

After second dose

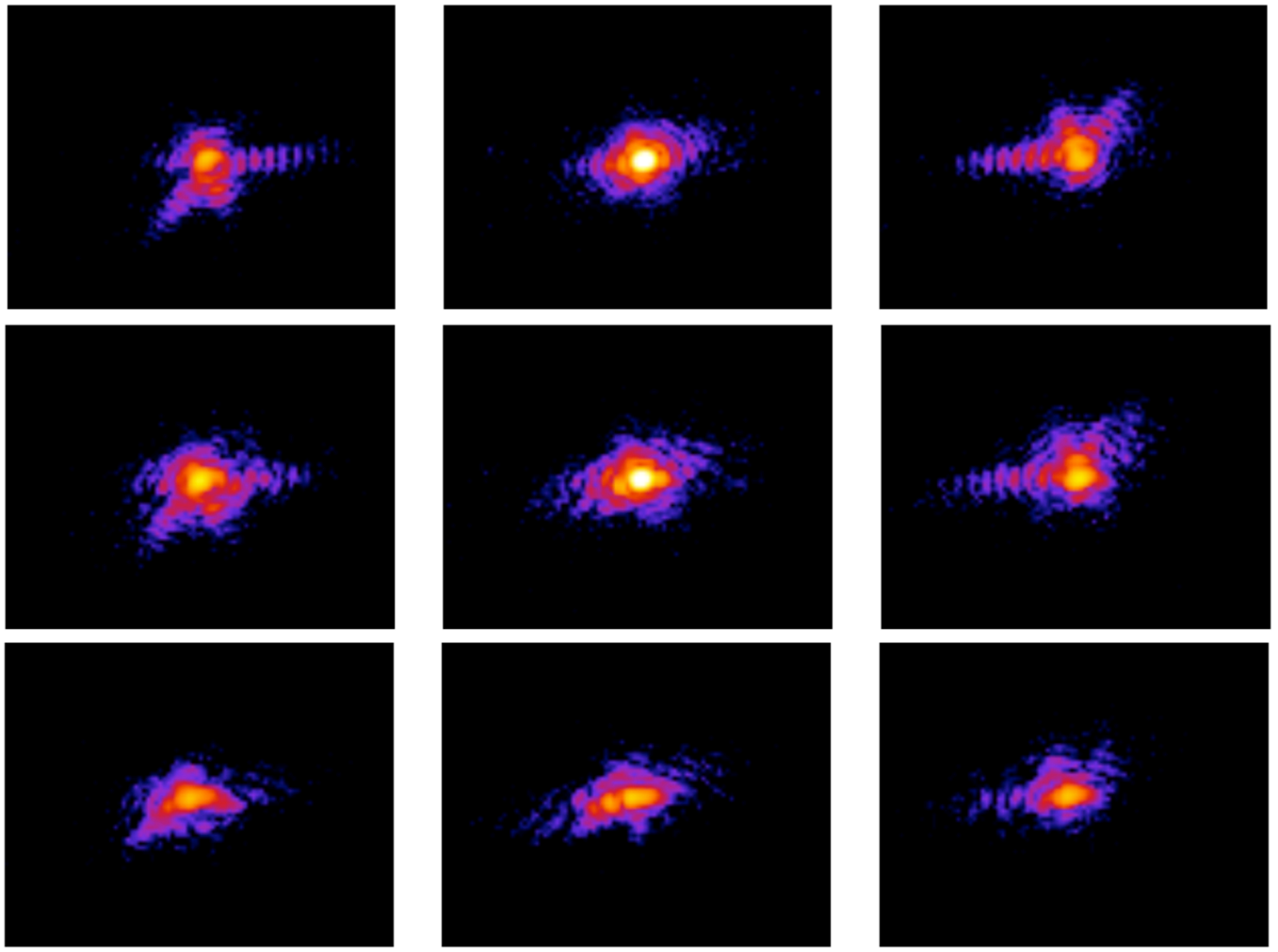

$\delta\omega=-0.025°$ $\delta\omega=0$ $\delta\omega=+0.025°$

Amplitude: xz-cut plane, T=400°C

Before Fe dose

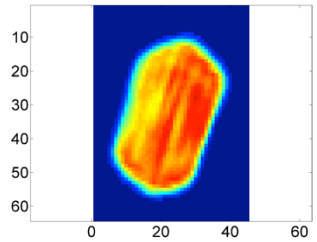

After 1st Fe dose,

t=10min

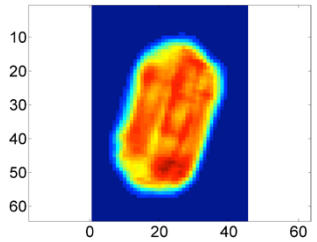

t=1hr

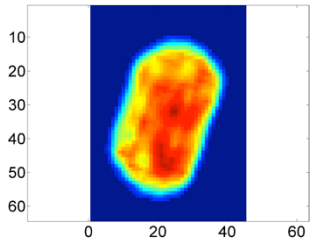

t=2hrs

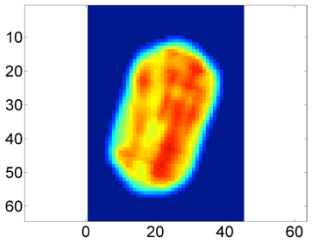

t=3hrs

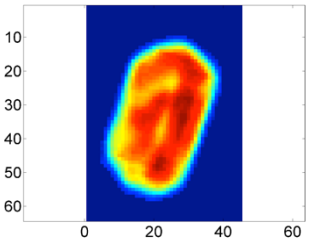

After 2nd Fe dose,

t=4hrs

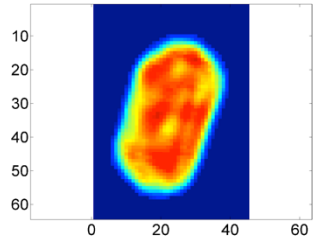

t=5hrs

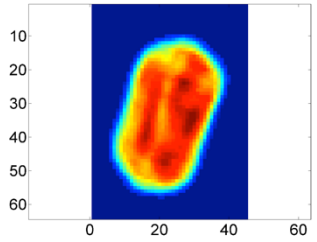

t=10min

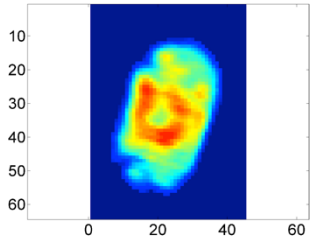

t=1hr

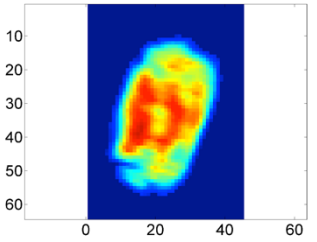

t=2hrs

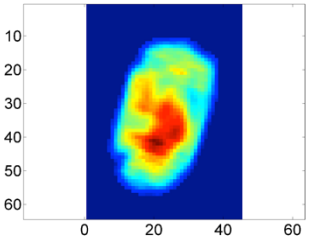

After 3rd Fe dose,

t=3hrs

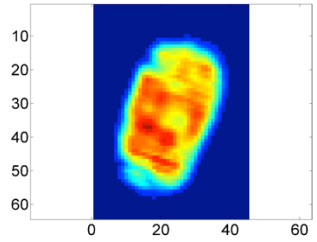

t=6hrs

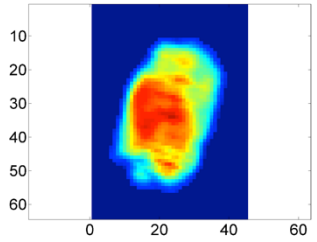

t=20min

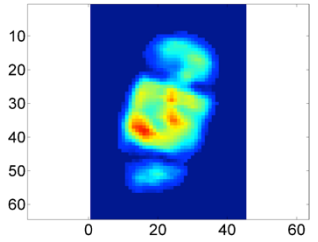

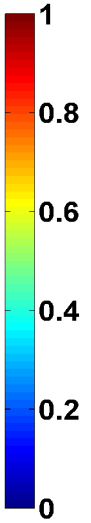

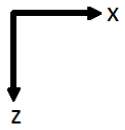

667 nm

I. K. Robinson, Soleil 2018

Phase: xz-cut plane, T=400°C

Before Fe dose

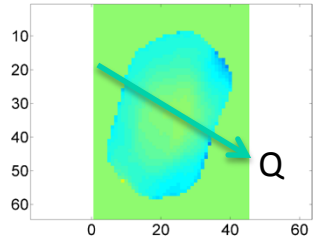

After 1st Fe dose,

t=10min

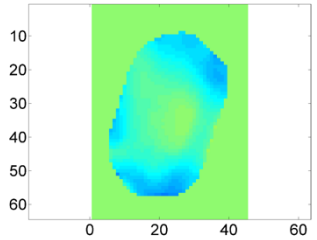

t=1hr

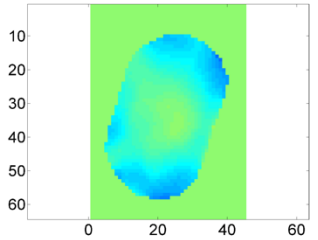

t=2hrs

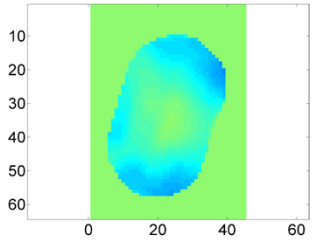

t=3hrs

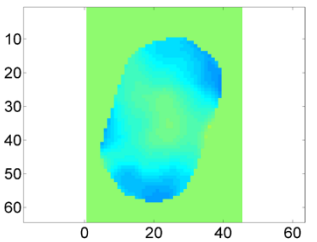

After 2nd Fe dose,

t=4hrs

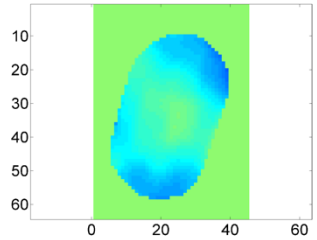

t=5hrs

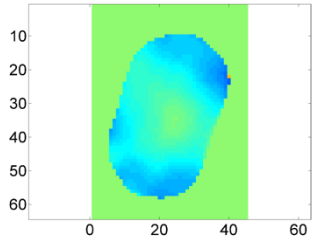

t=10min

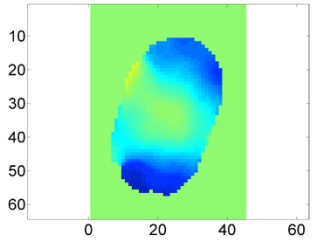

t=1hr

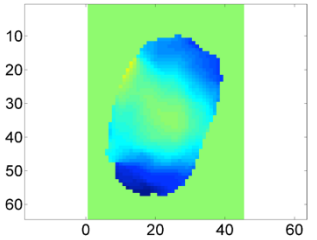

t=2hrs

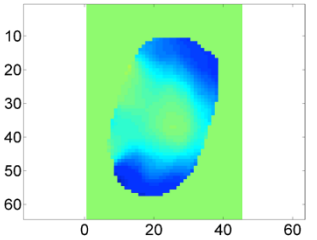

After 3rd Fe dose,

t=3hrs

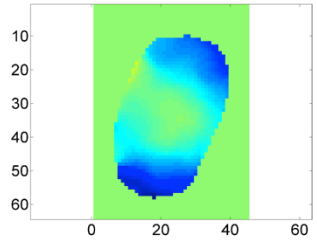

t=6hrs

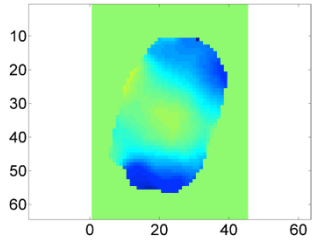

t=20min

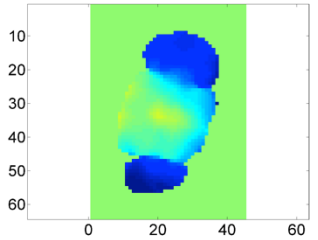

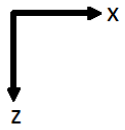

667 nm

xy- and zy-cut planes, T=400°C

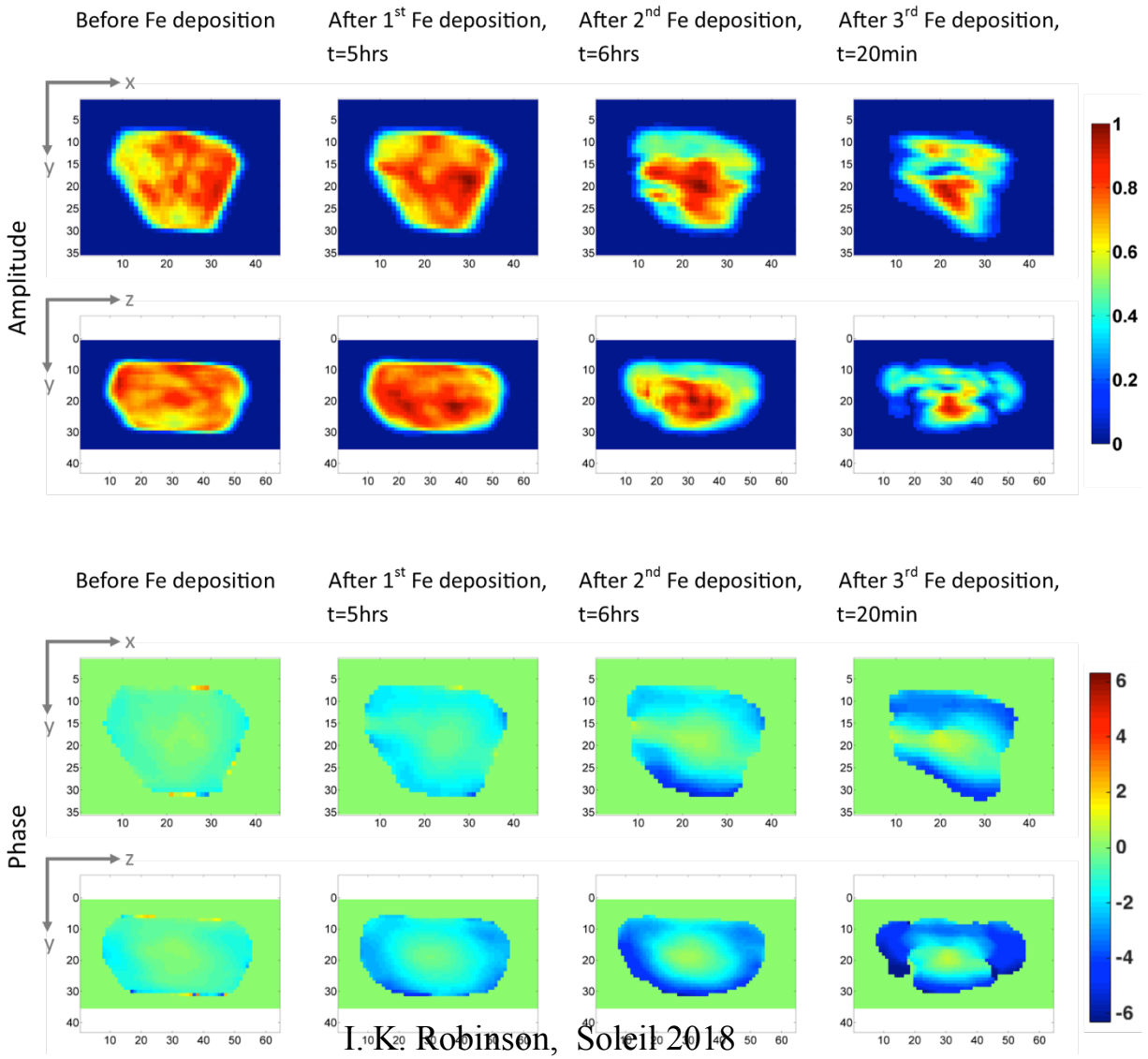

Phase Isosurface Images

Control

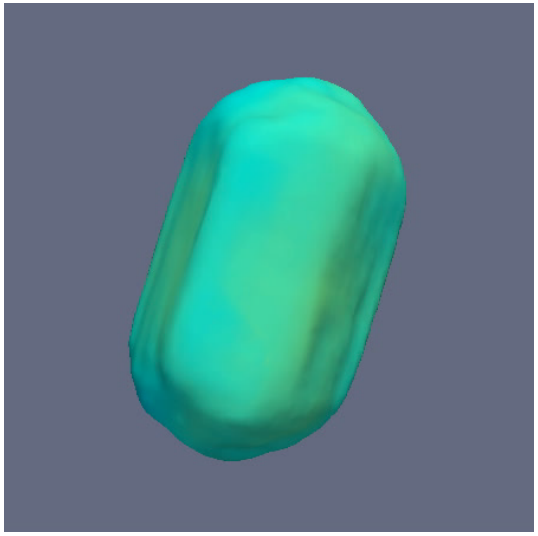

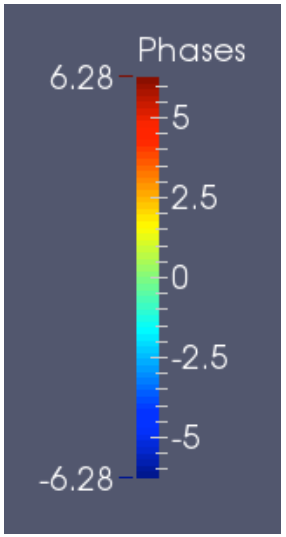

After 1st Fe dose

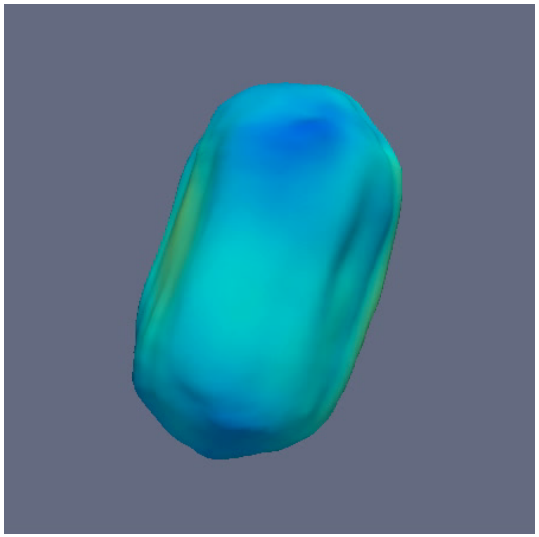

After 2nd Fe dose

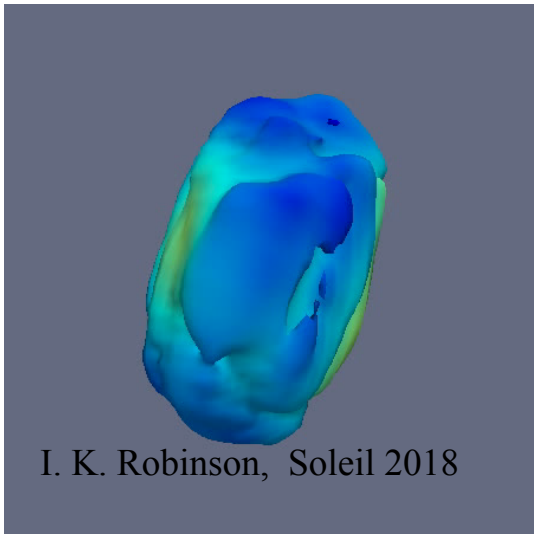

After 3rd Fe dose

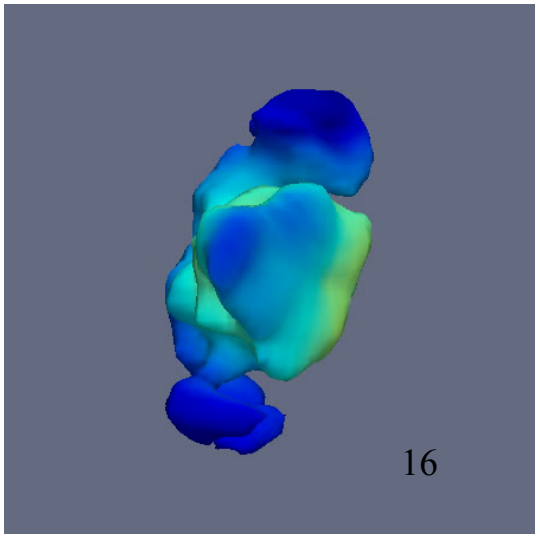

Amplitude and Phase, T=300°C

Ana Estandarte, to be published

Before Fe dose

1st Fe dose, t=6hrs

2st Fe dose, t=8hrs

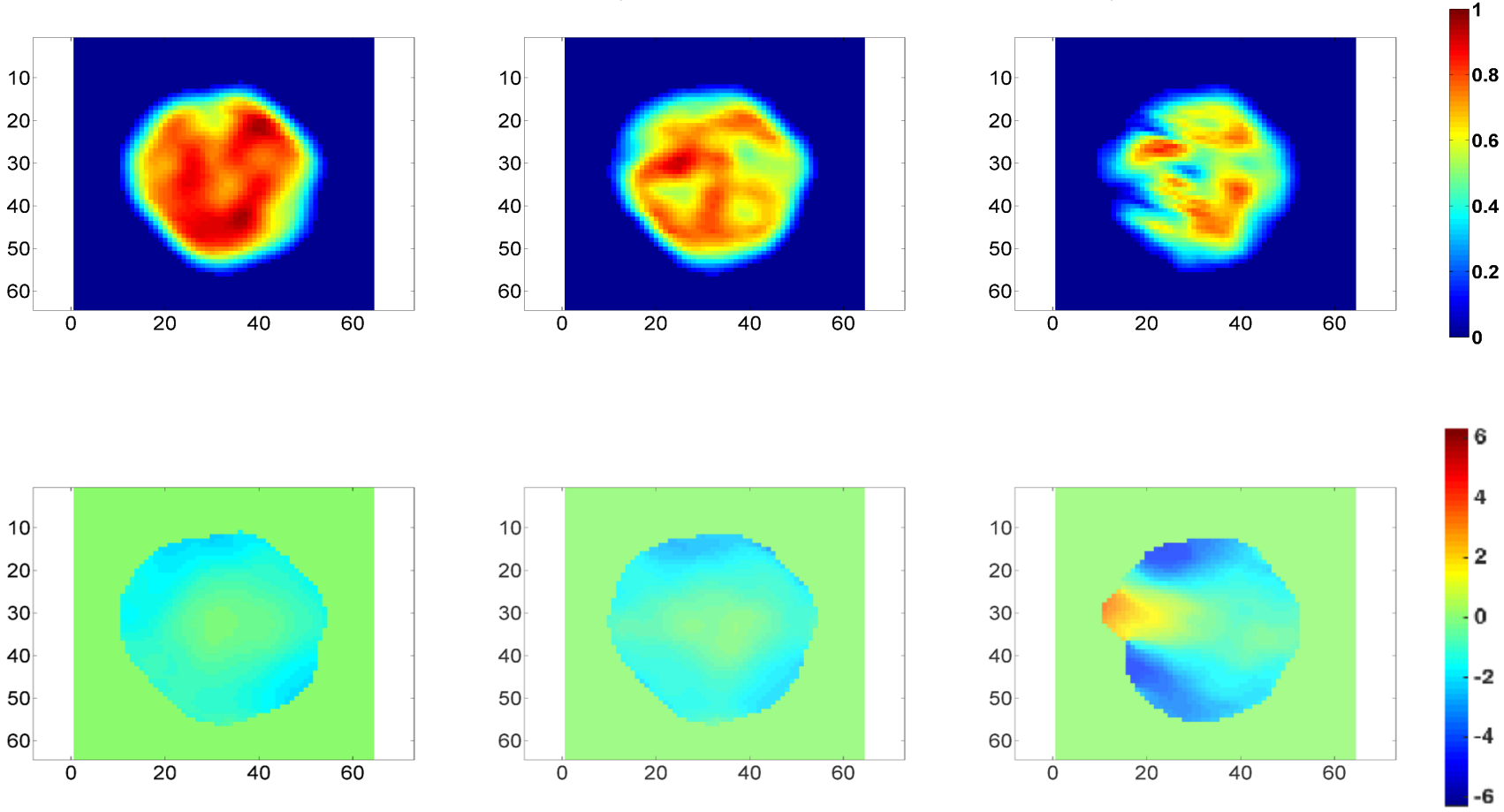

Misfit Dislocations and Stacking Faults

Ana Estandarte, to be published

- Alloying of Fe with Au → contraction of the nanocrystal lattice
- Lattice misfit between AuFe shell and Au core → formation of misfit dislocations

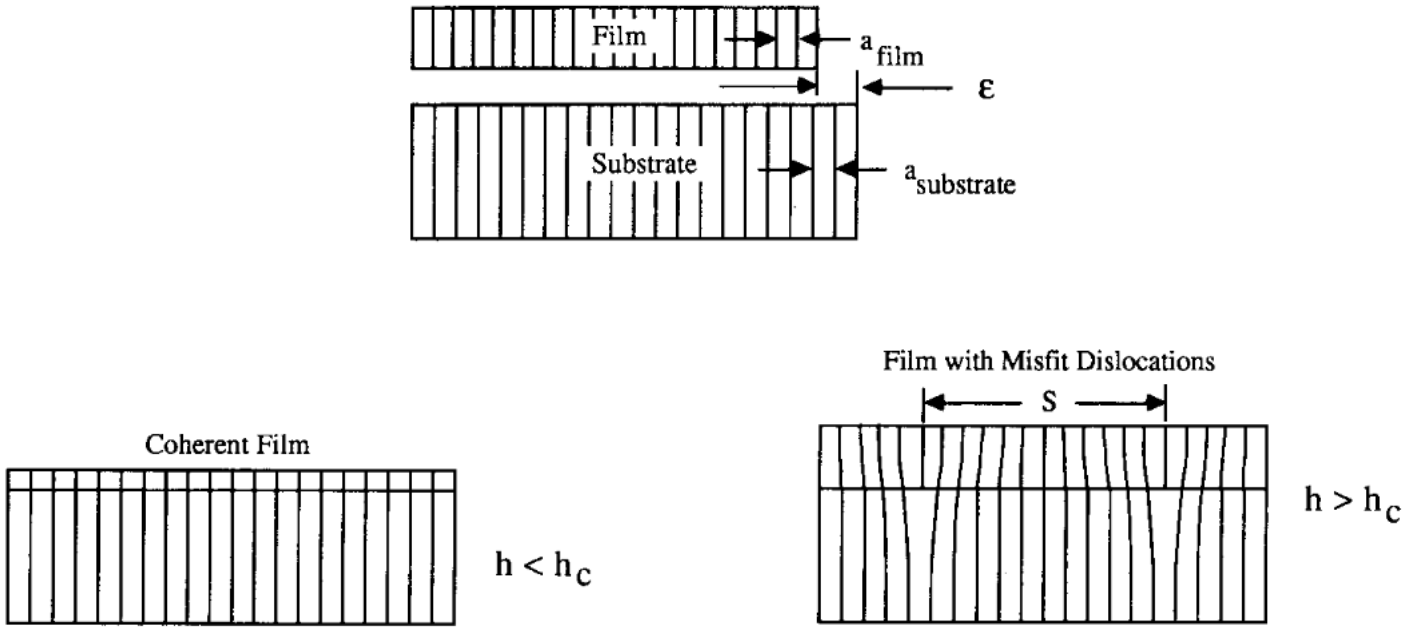

Phase cross sections vs dosing

Transverse

Along Q-vector

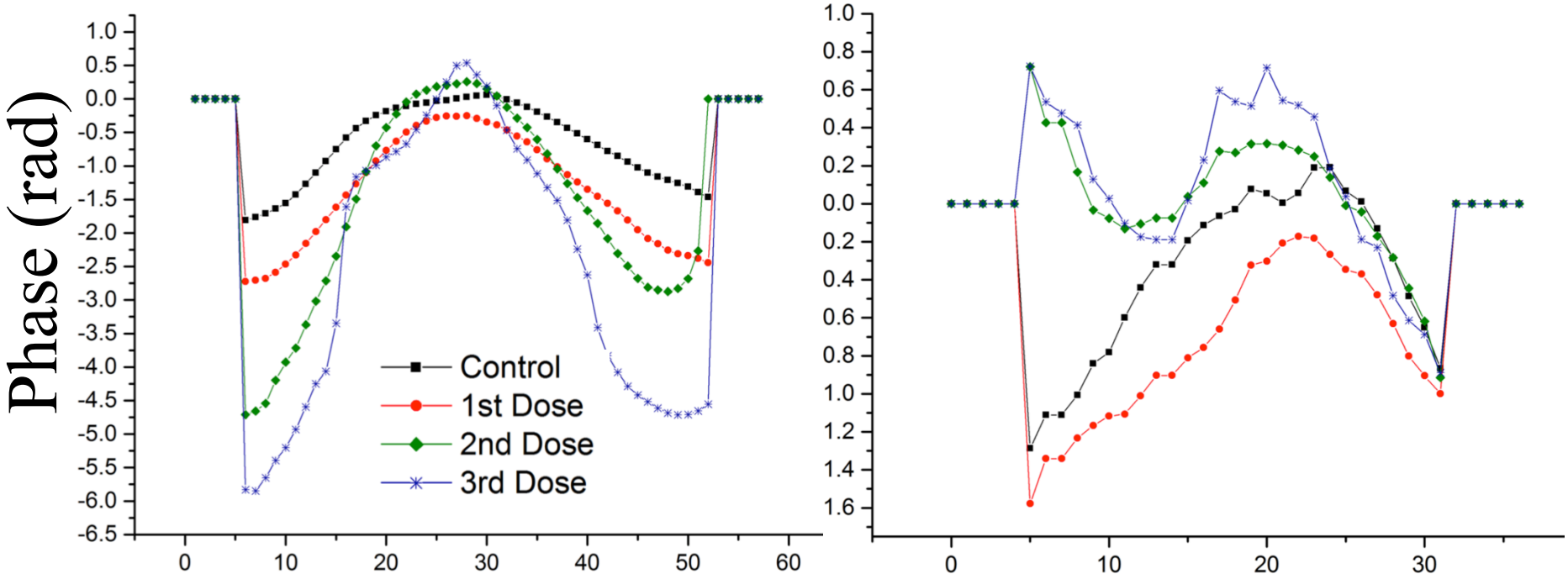

Distance (pixels)

Schematic of displacements in Fe/Au nanoparticles

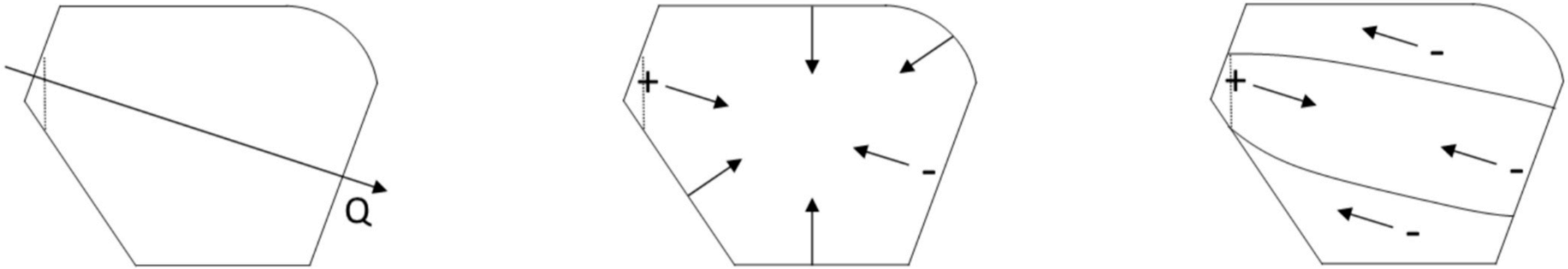

$La_{0.5}Ca_{0.5}MnO_3$ (LCMO) nanocrystals

SEM by Xiaojing Huang

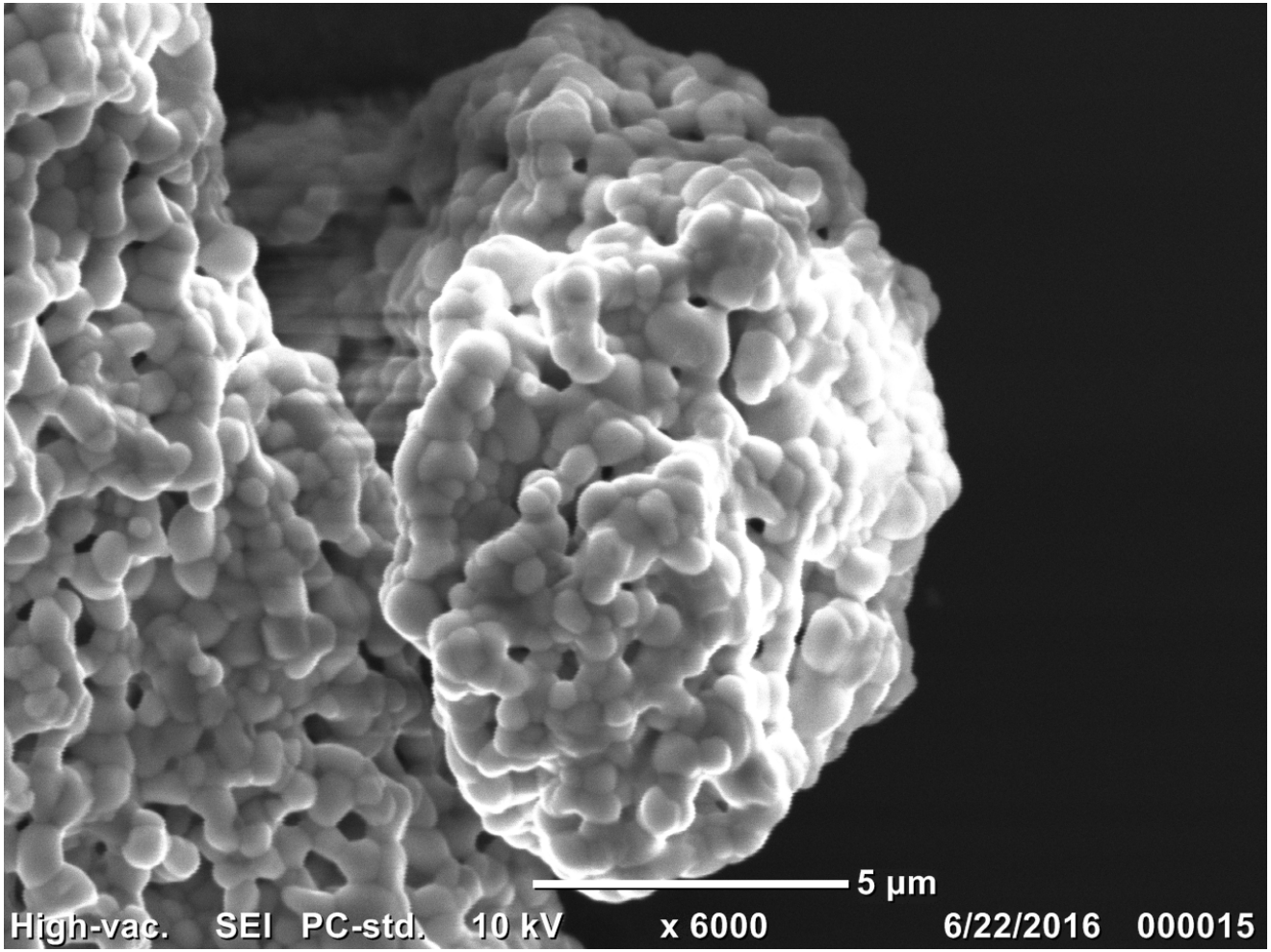

Colossal Magnetoresistance (CMR)

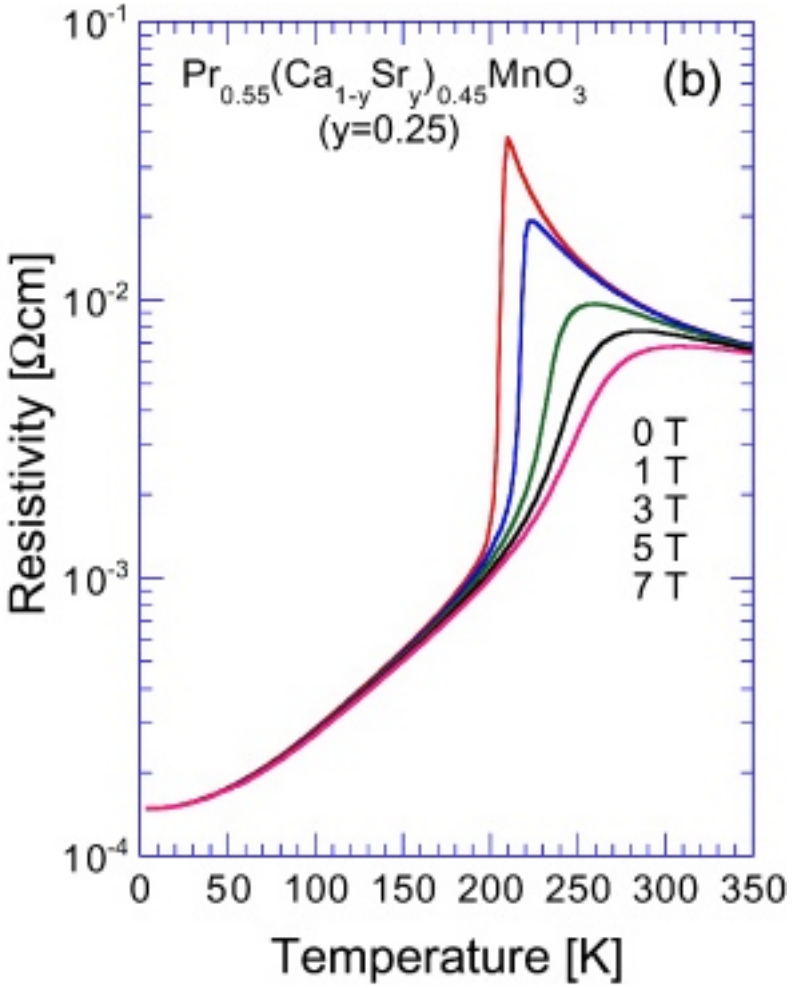

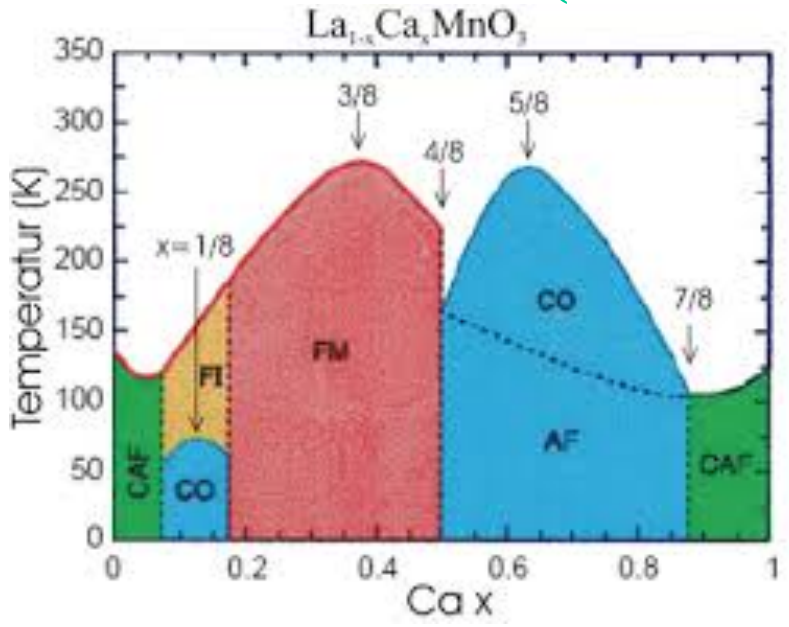

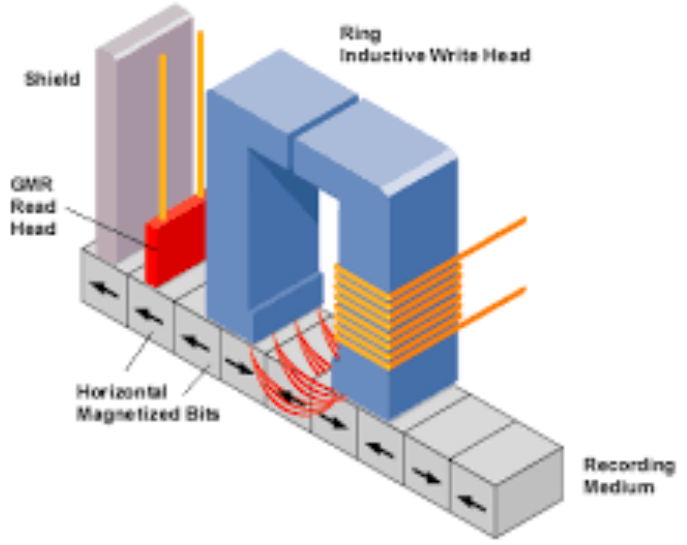

I. K. Robinson,

BCDI Images from LCMO-500

Phase Domain structure

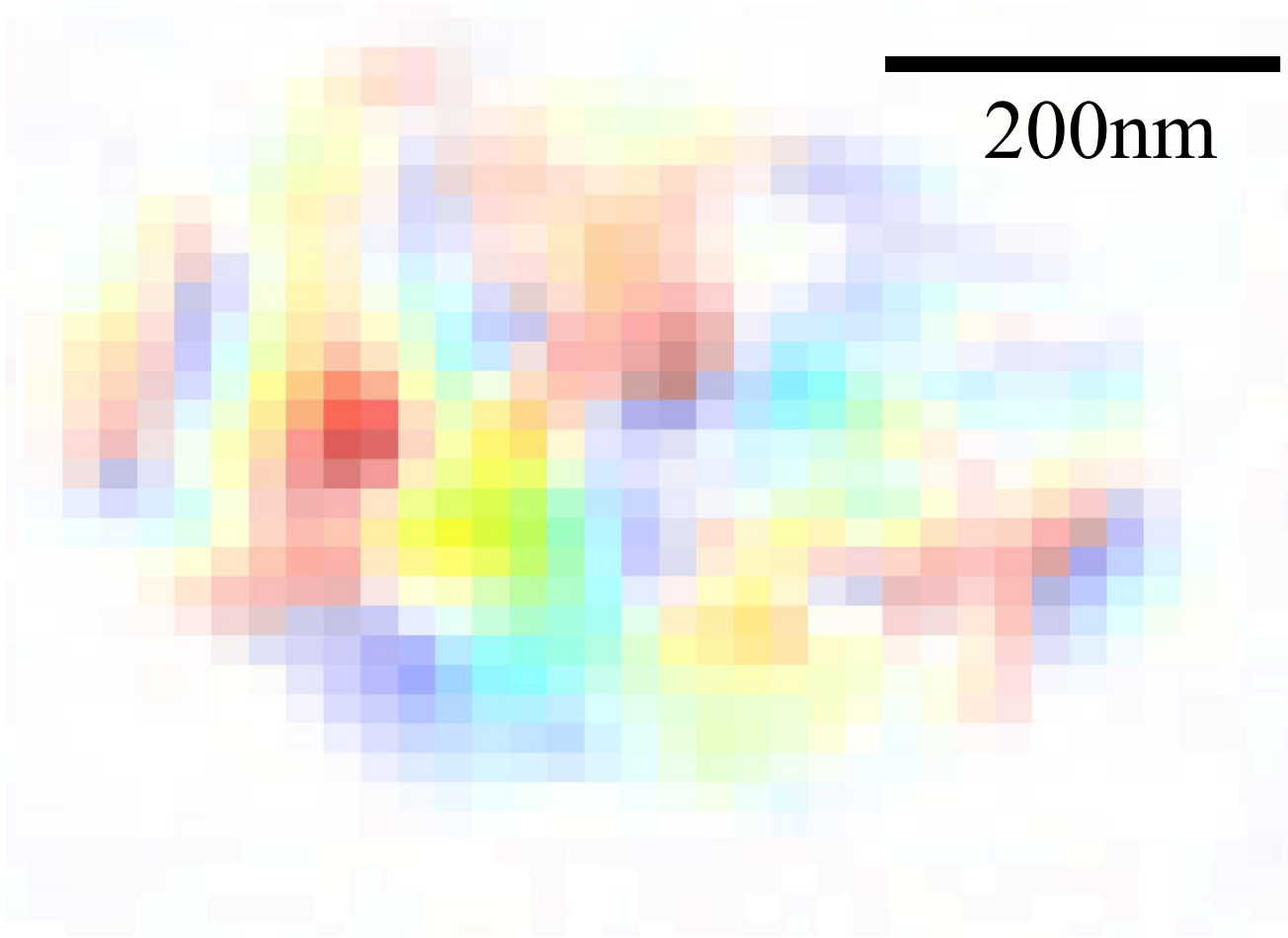

$La_{0.5}Ca_{0.5}MnO_3$ Phase Domains

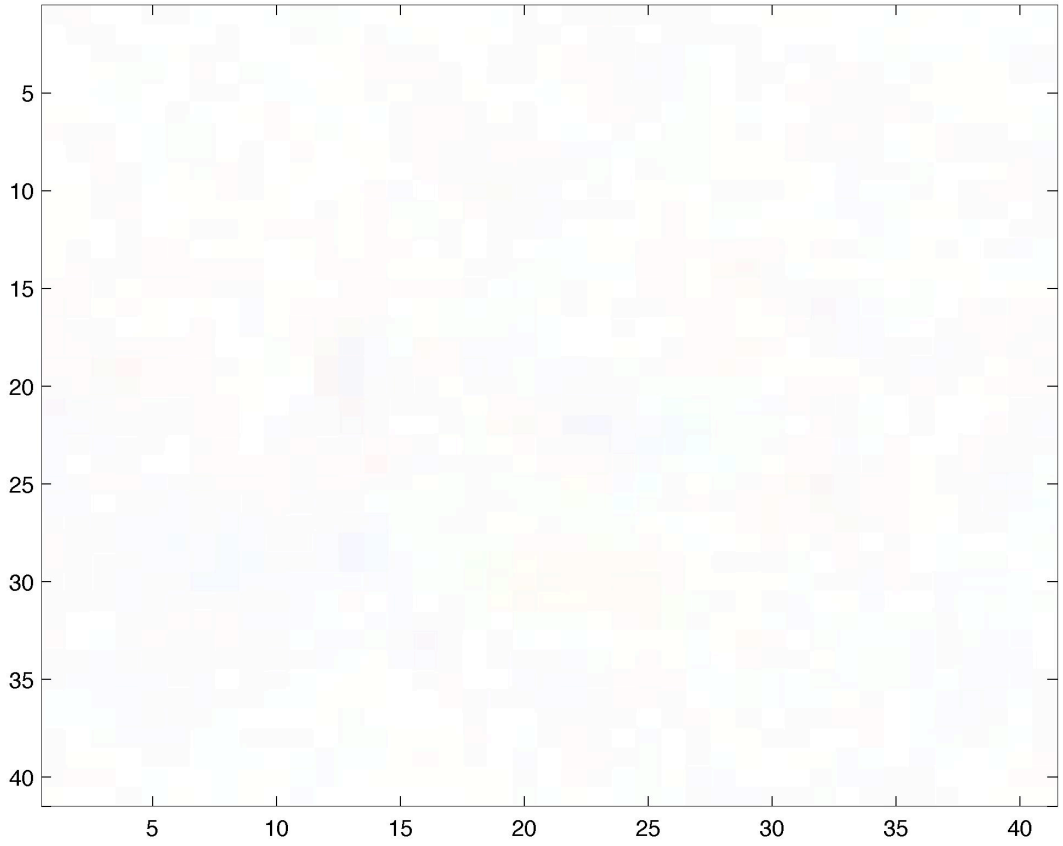

Hue Saturation Value (HSV) coding for complex images

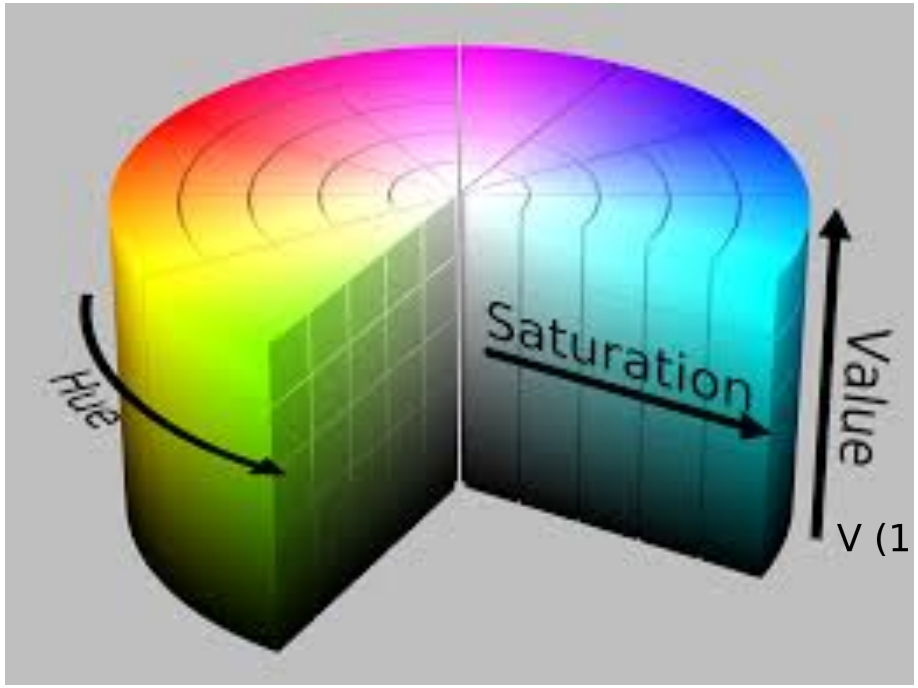

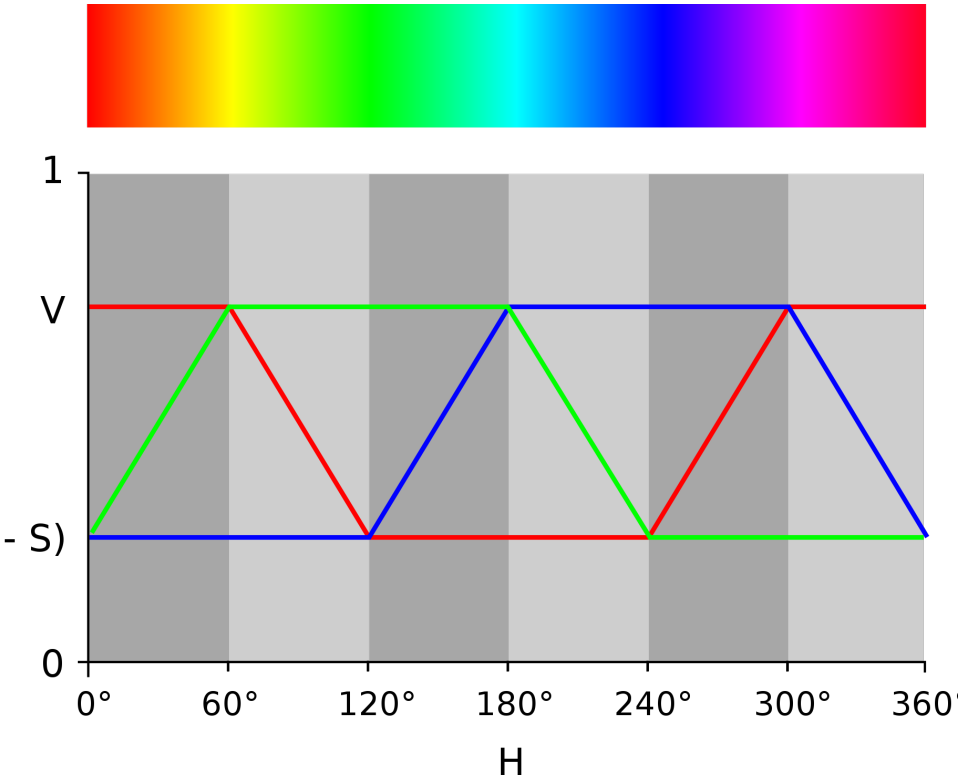

Zero-angle grain boundary

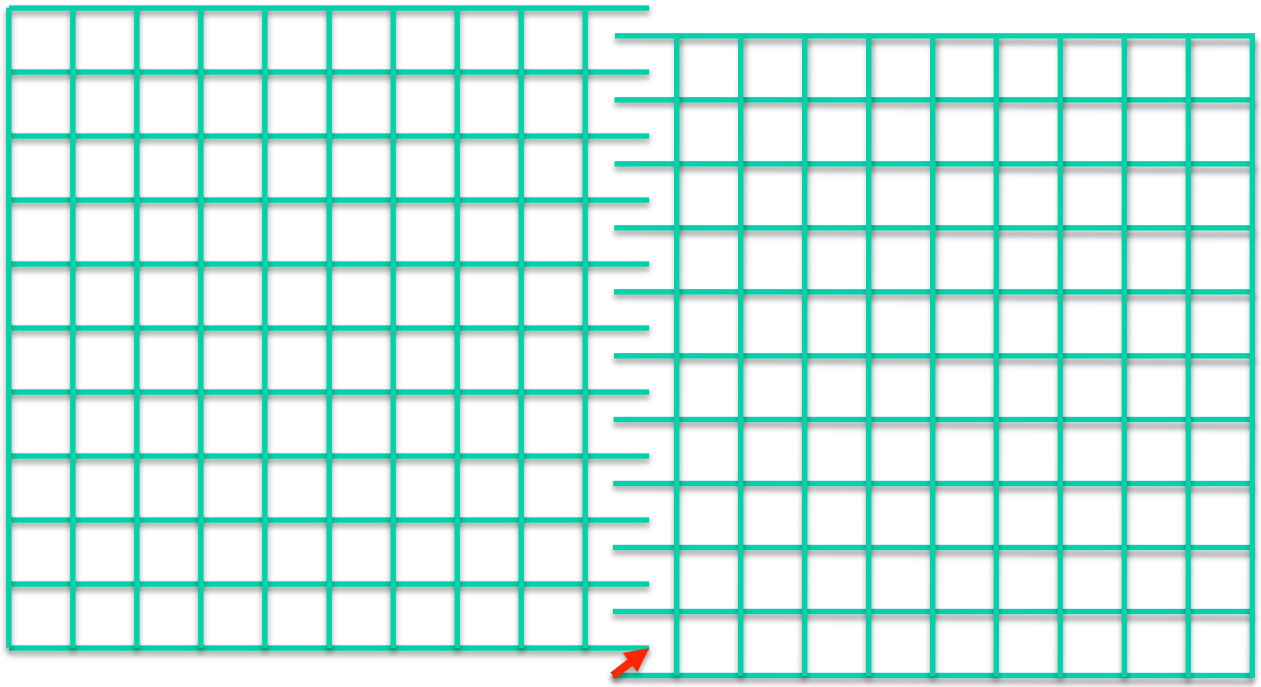

- Each domain has a Phase, relative to a reference lattice
- Phase shift depends on measurement vector **Q**
- Phase boundaries contribute to crystal “mosaic”

$BaTiO_3$ bicrystal imaged by BCDI

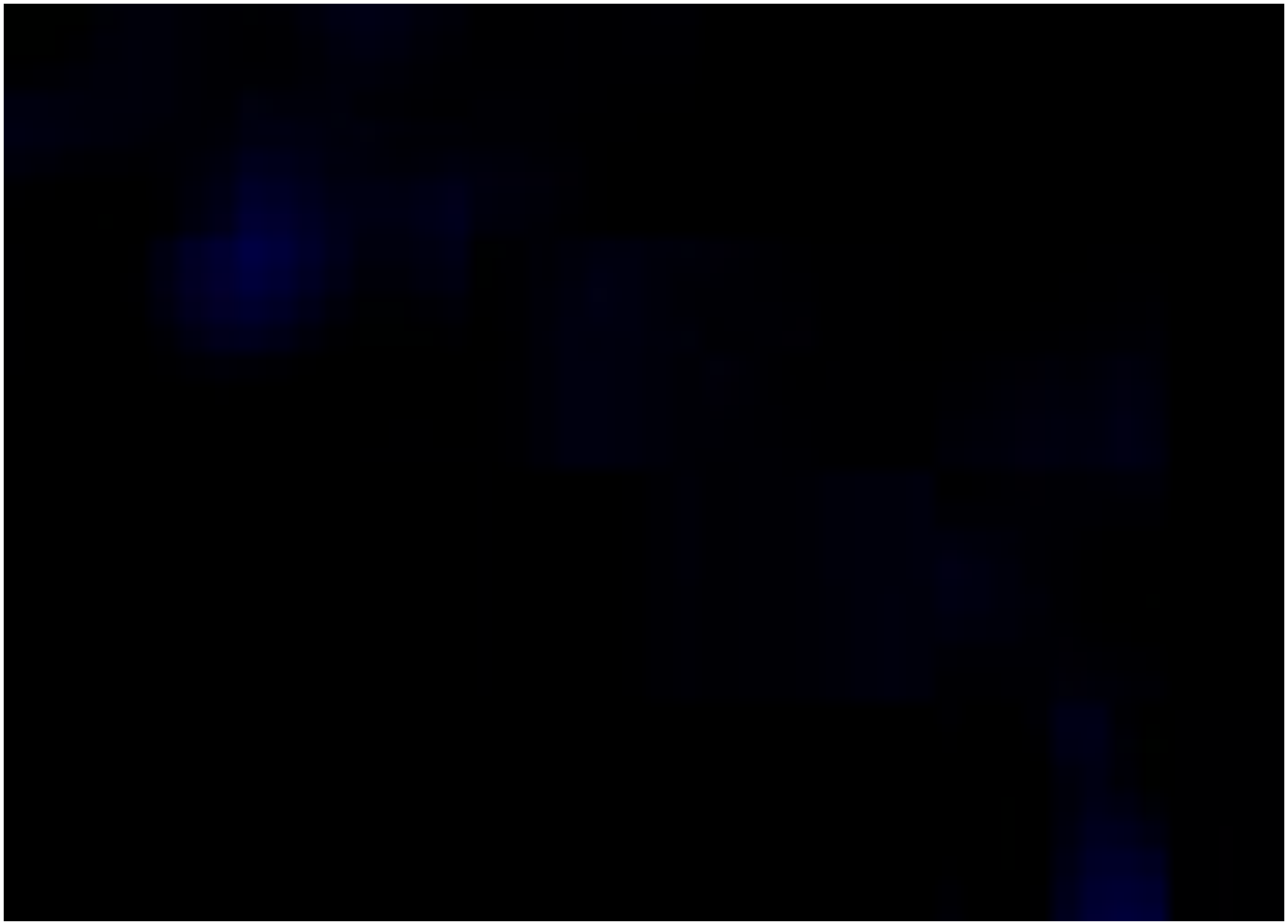

BCDI from Barium Titanate ($BaTiO_3$)

34-ID-C

APS

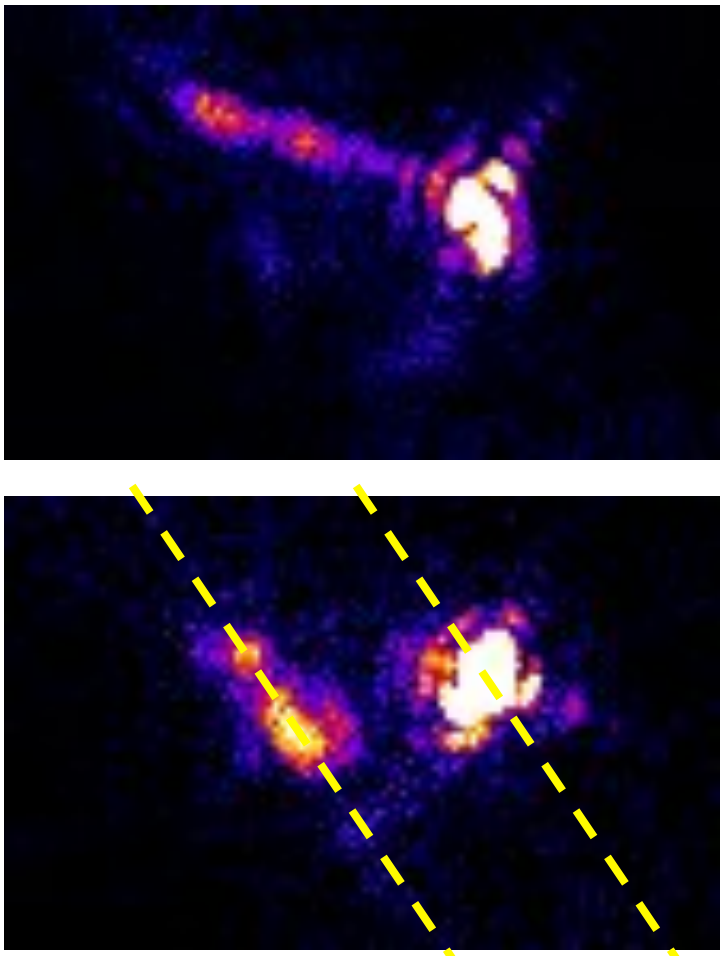

Tetragonal splitting

BCDI from Barium Titanate (BTO)

3D reconstruction #312 shows merohedral twinning

M. A. G. Aranda et al, JSR 17 751 (2010)

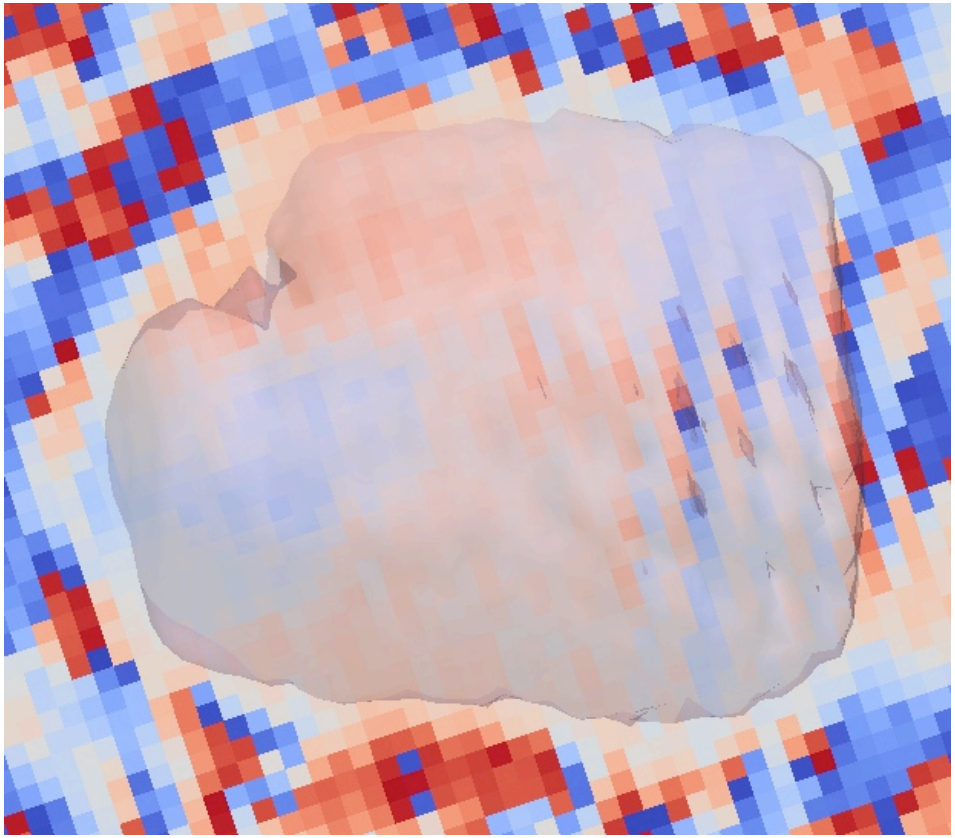

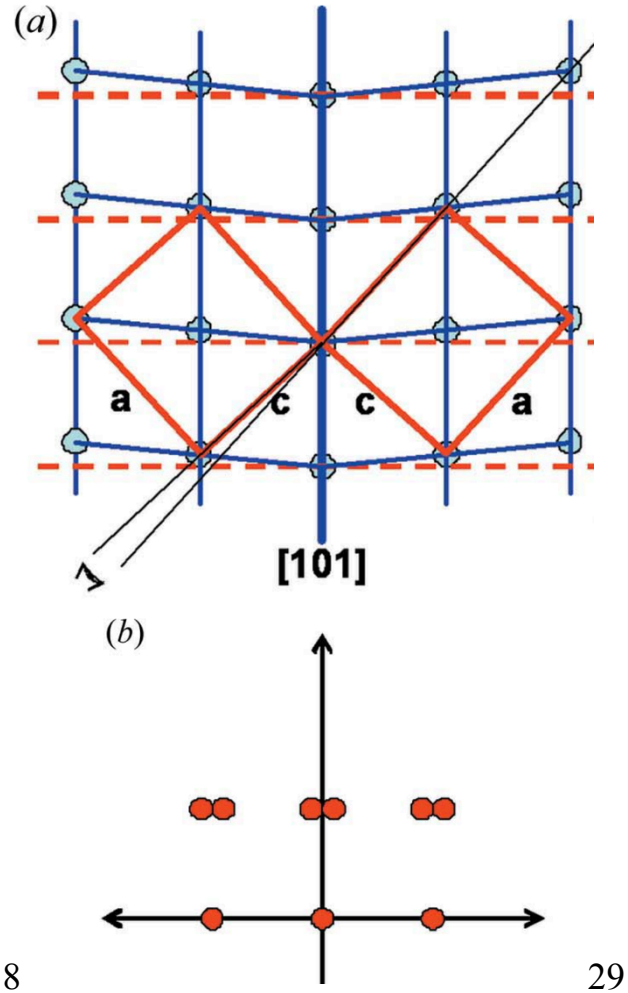

Twinned quartz crystals

Twinning seen as phase ramps in BCDI

M. A. G. Aranda et al, JSR **17** 751 (2010)

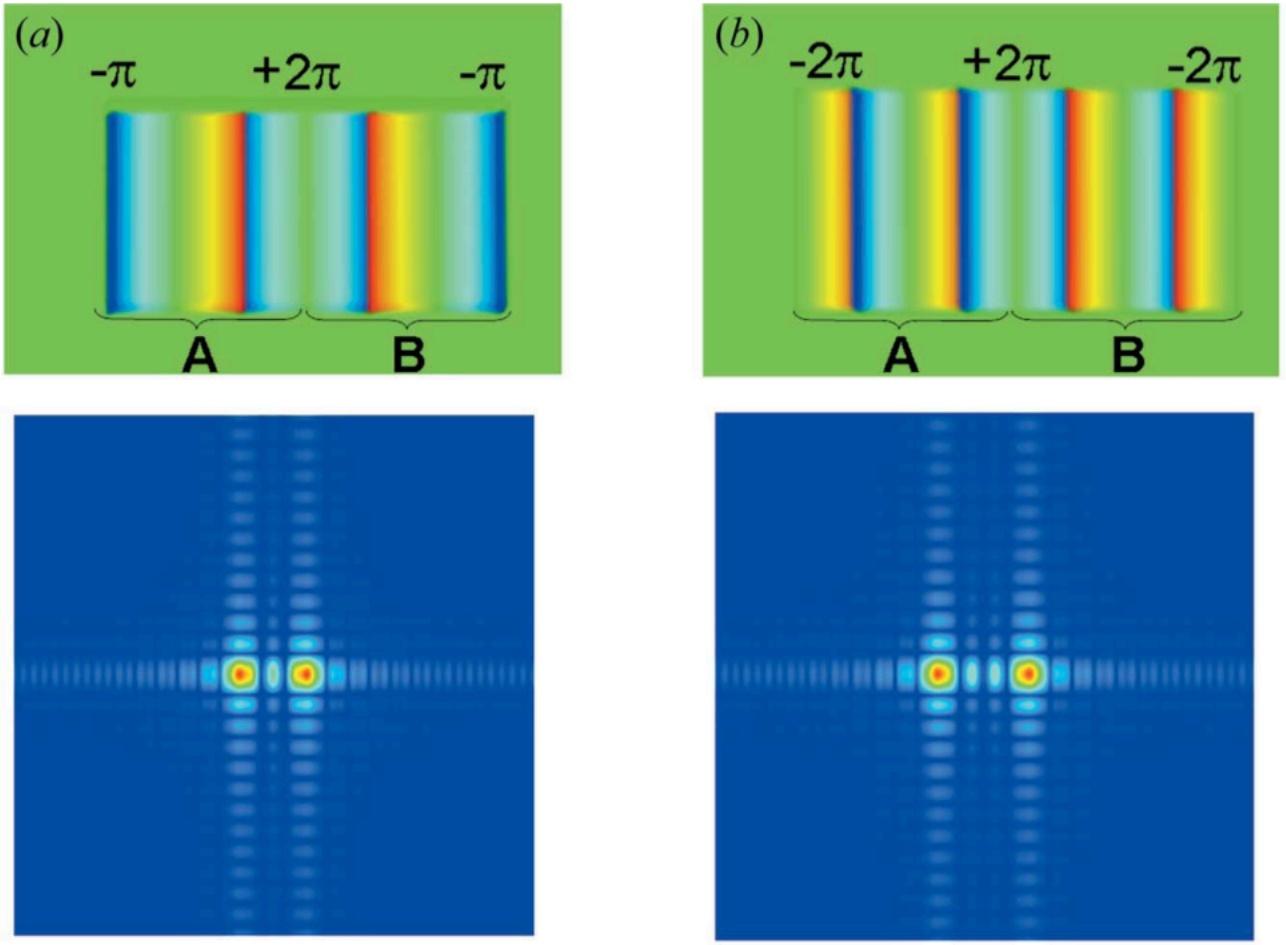

Coherent Soft X-ray Scattering (CSX-1)

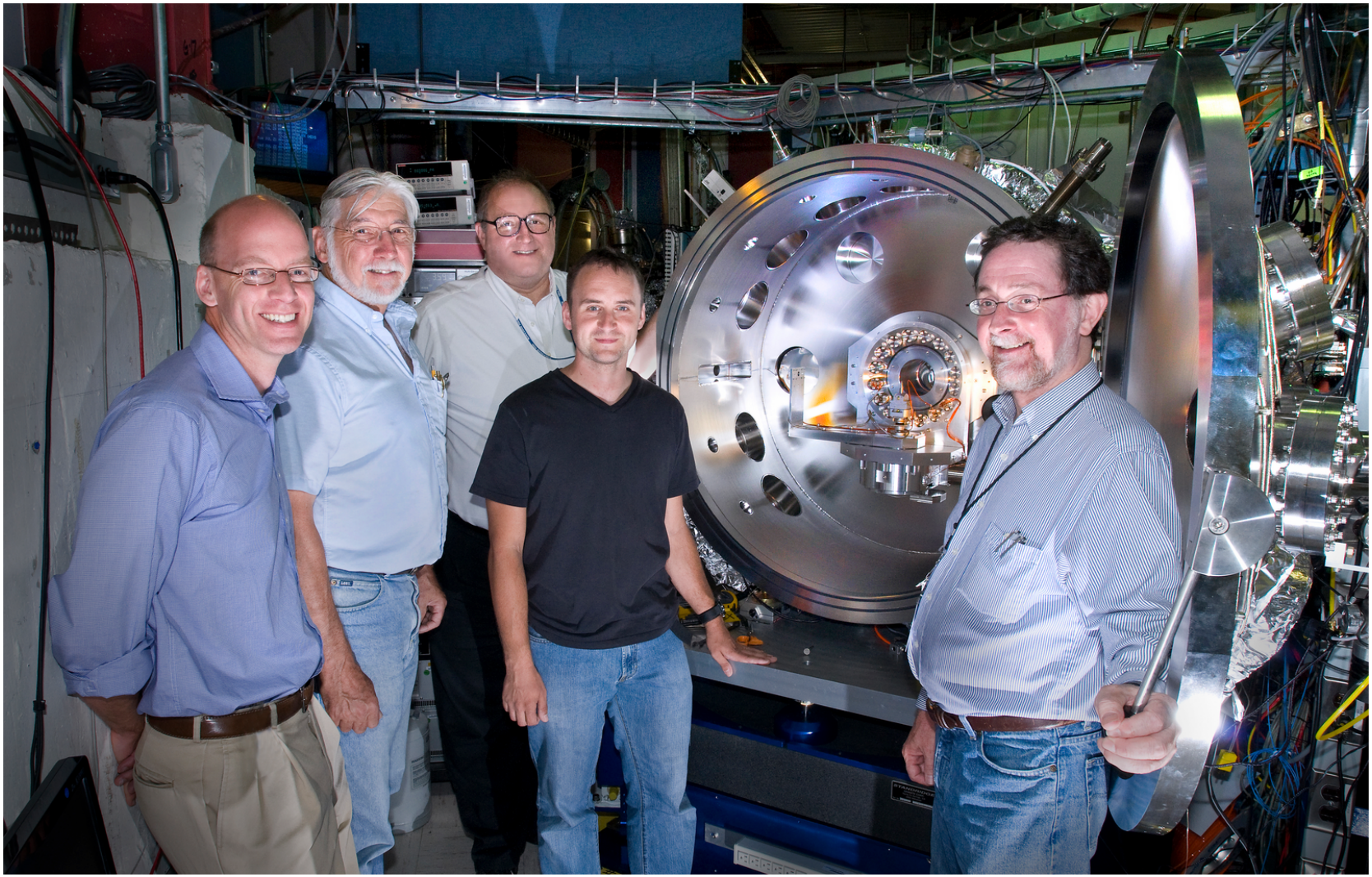

High Temperature Superconductor, $La_{2-x}Ba_xCuO_4$

Subir Sachdev, Trans Roy Soc

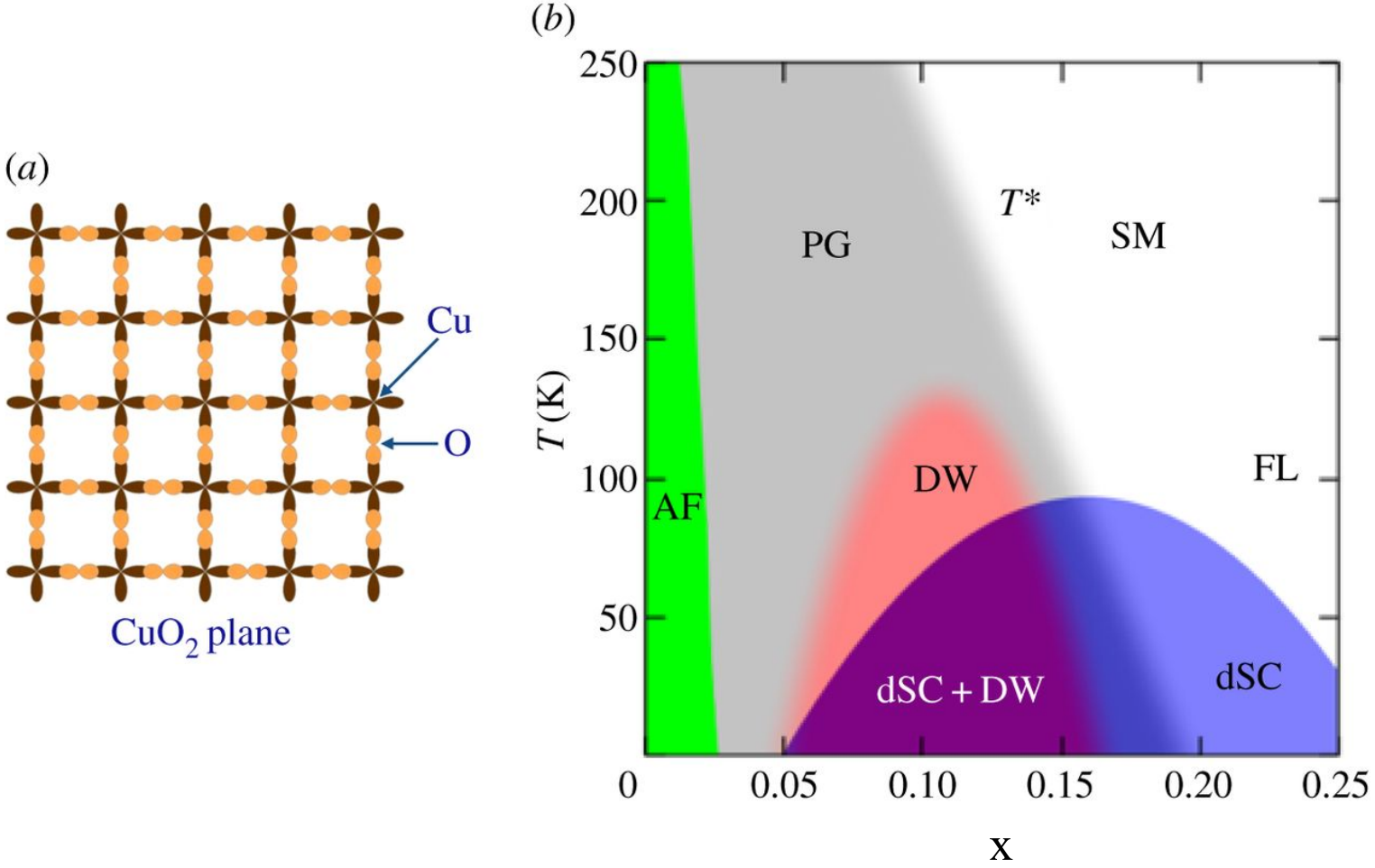

HTT-LTO-LTT phases of $La_{2-x}Ba_xCuO_4$

G. Fabbris et al, Phys. Rev B 88 060507 (2013)

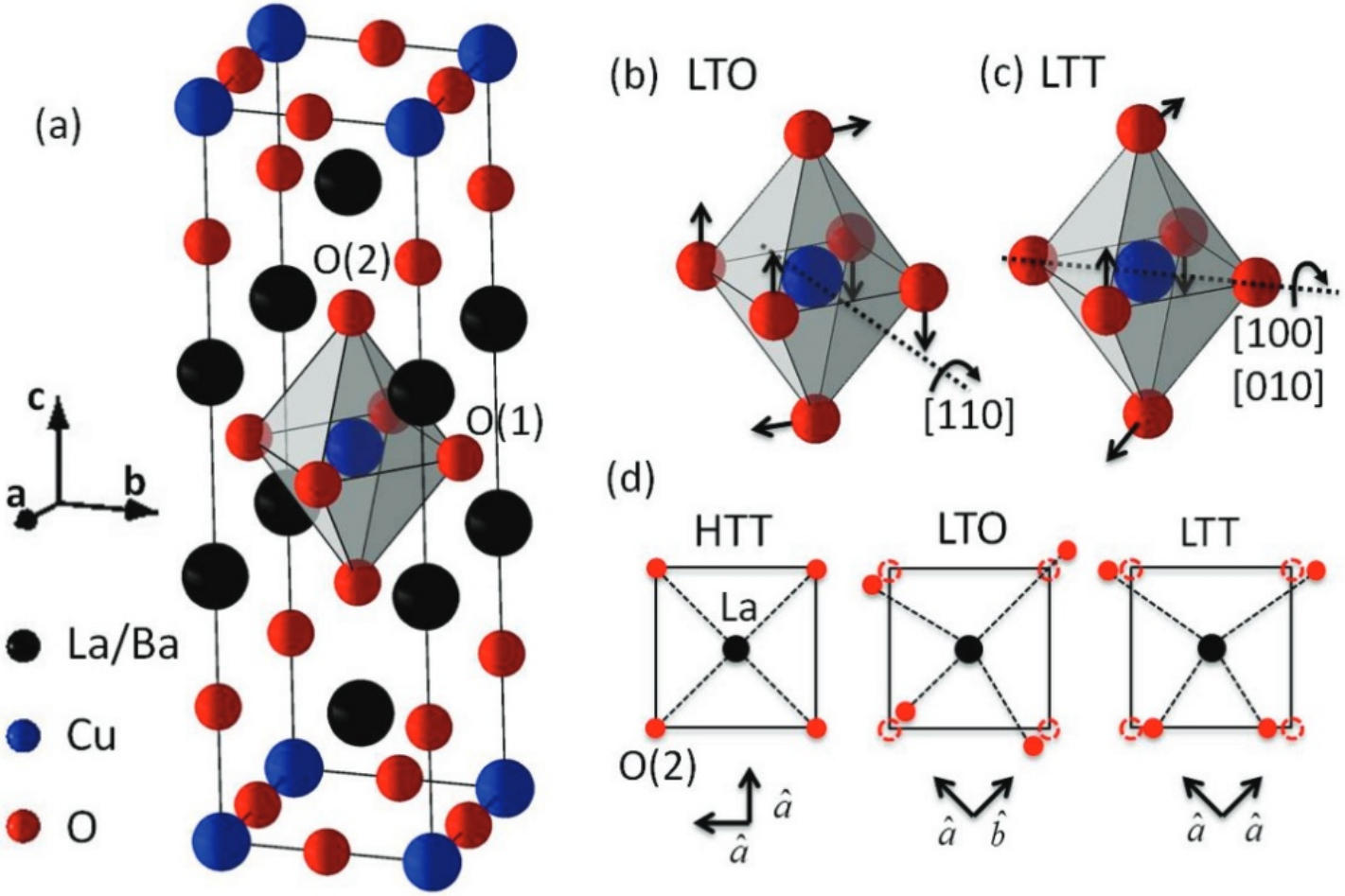

Stripes with Doping $La_{2-x}Ba_xCuO_4$

M. Hucker et. al., Phys. Rev. B **83** 104506 (2011)

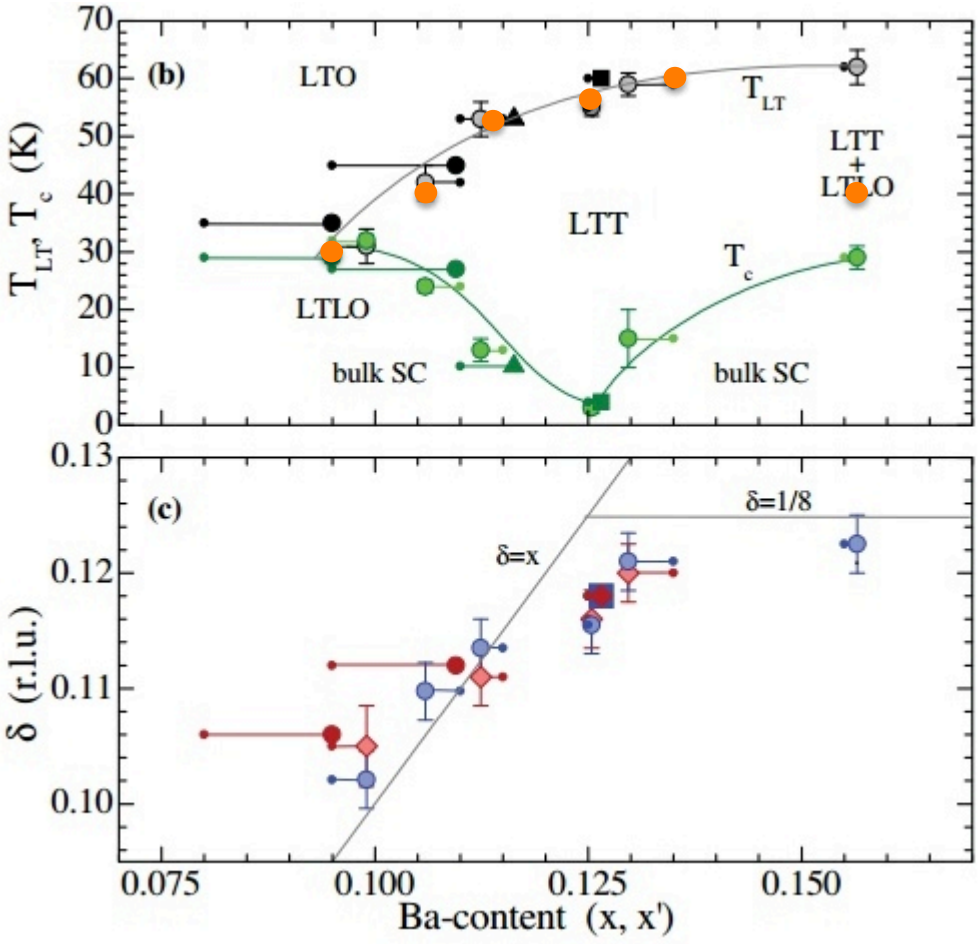

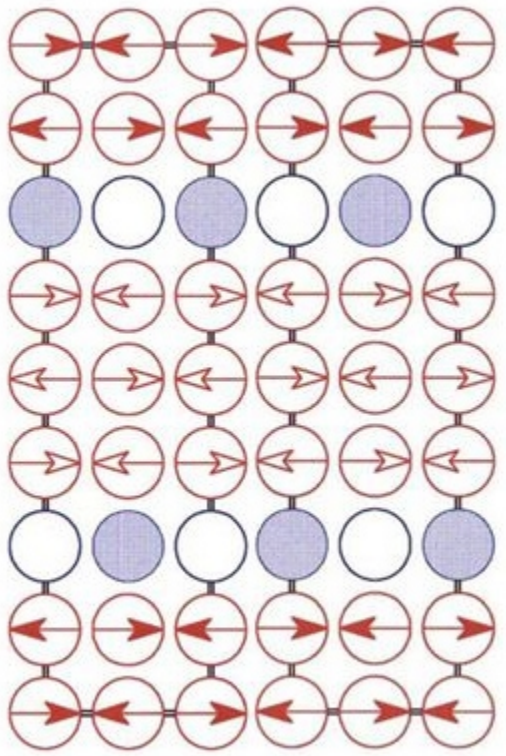

$La_{1.875}Ba_{0.125}CuO_4$ "stripe" fluctuations

X.M. Chen, V. Thampy, C. Mazzoli, A. M. Barbour, H. Miao, G.D. Gu, Y. Cao, J. M. Tranquada, M. P. M. Dean and S. B. Wilkins, Phys. Rev. Letts. 117 167001 (2016)

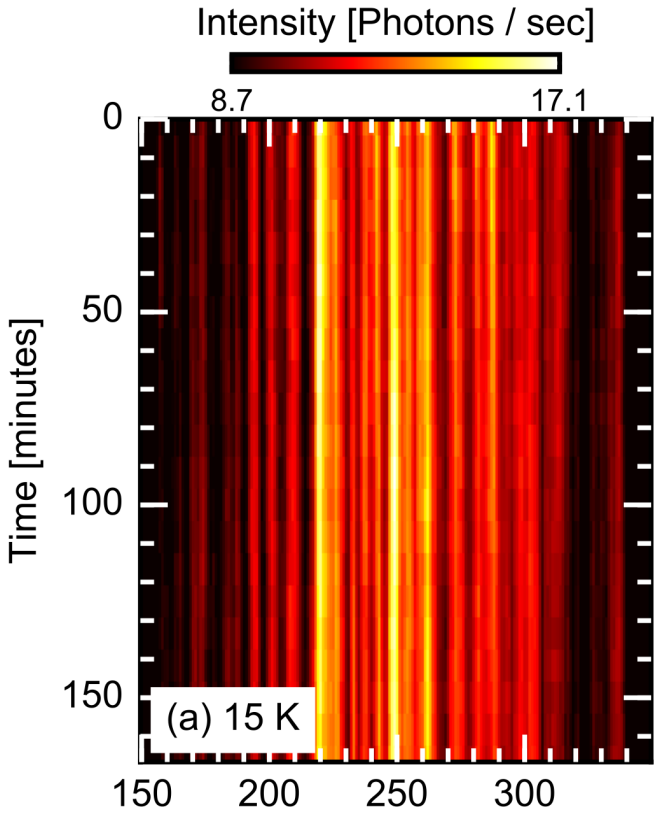

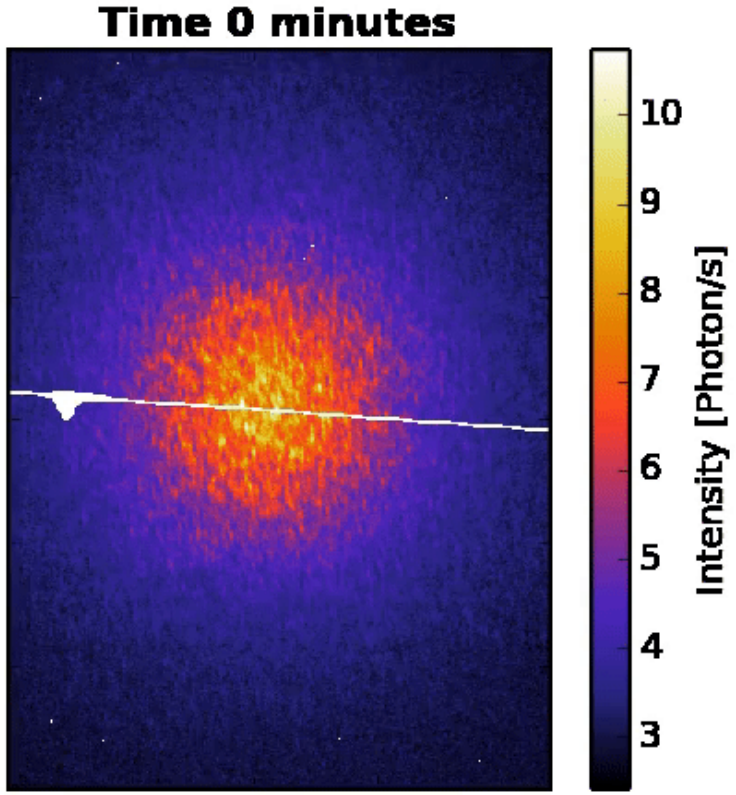

$La_{1.875}Ba_{0.125}CuO_4$ pinning persistence

NSLS-II CSX beamline

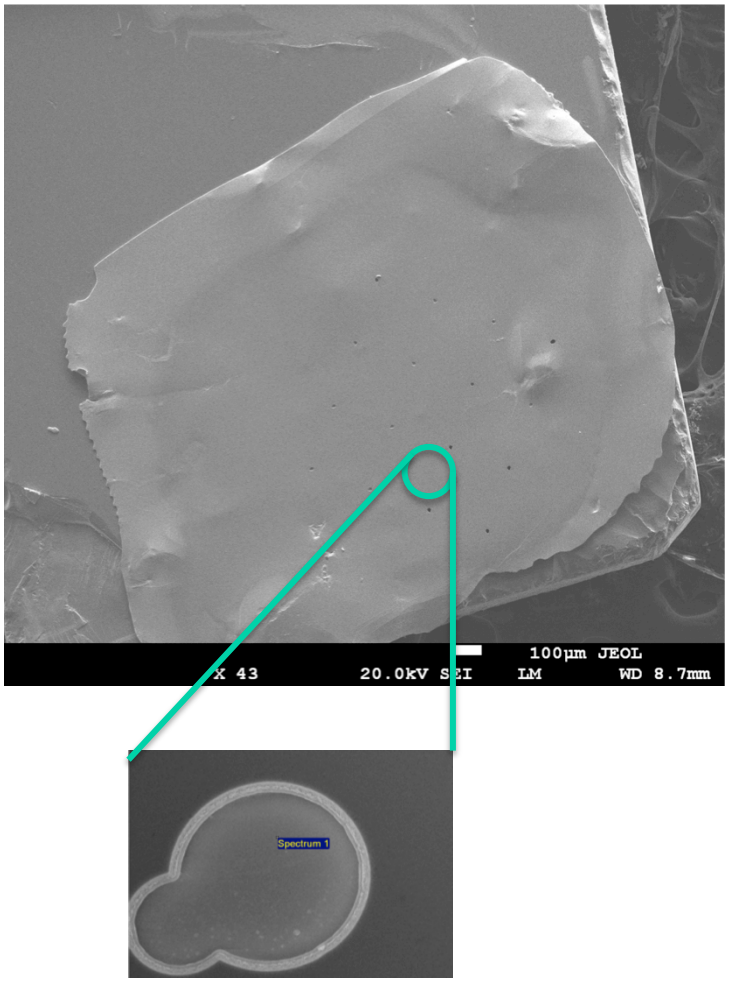

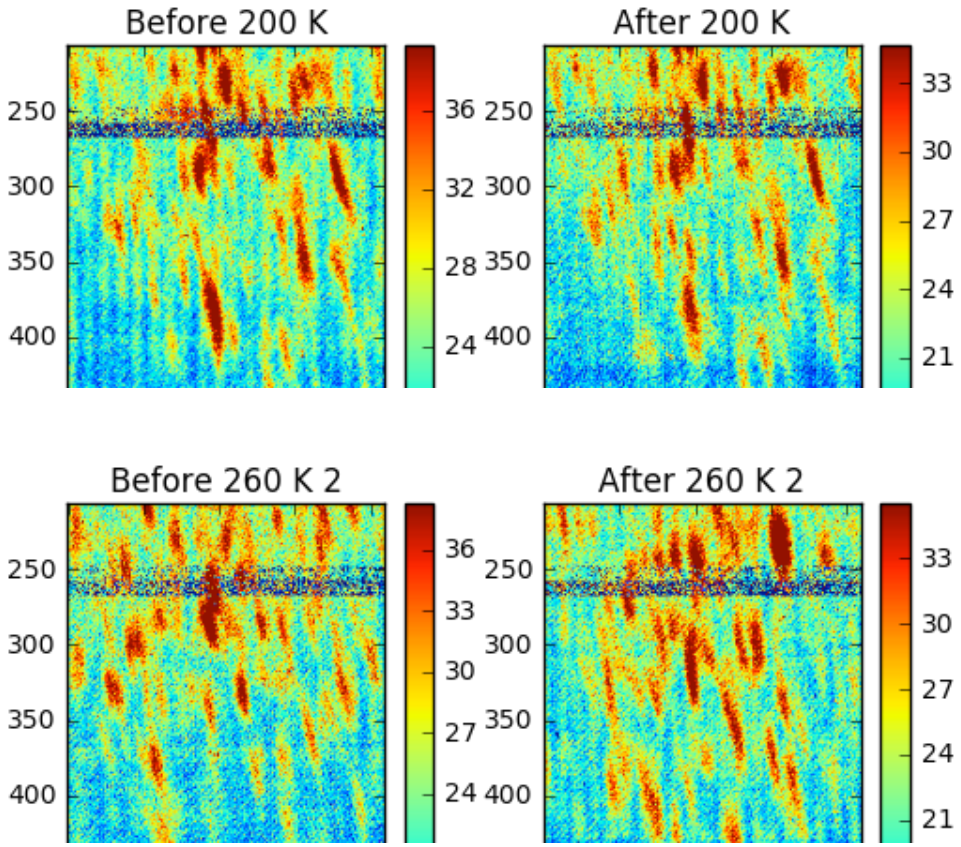

Temperature Excursion of LBCO Speckle

- Correlation before/after excursion calculated over central speckle region
- Conclude pinning of stripes is at orthorhombic LTO domain walls

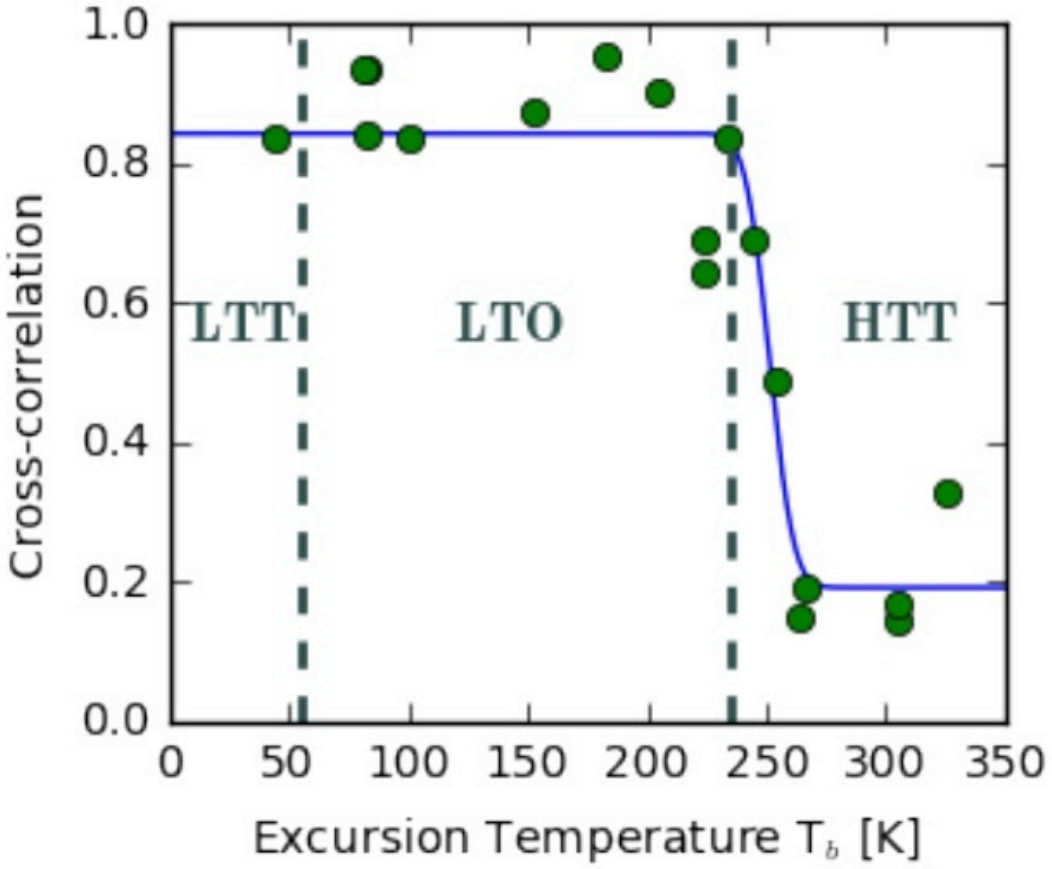

$La_{1.9}Sr_{0.1}CuO_4$ Domain Walls are LTT

- Y. Horibe, Y. Inoue, Y. Koyama, PRB **61** 11922 (2000); Yimei Zhu et al PRL **73** 3026 (1994)
- TEM Image of $La_{1.9}Sr_{0.1}CuO_4$ at 12K in LTO phase, imaged using (100) LTT peak
- 10nm of LTT phase in domain walls between LTO twins

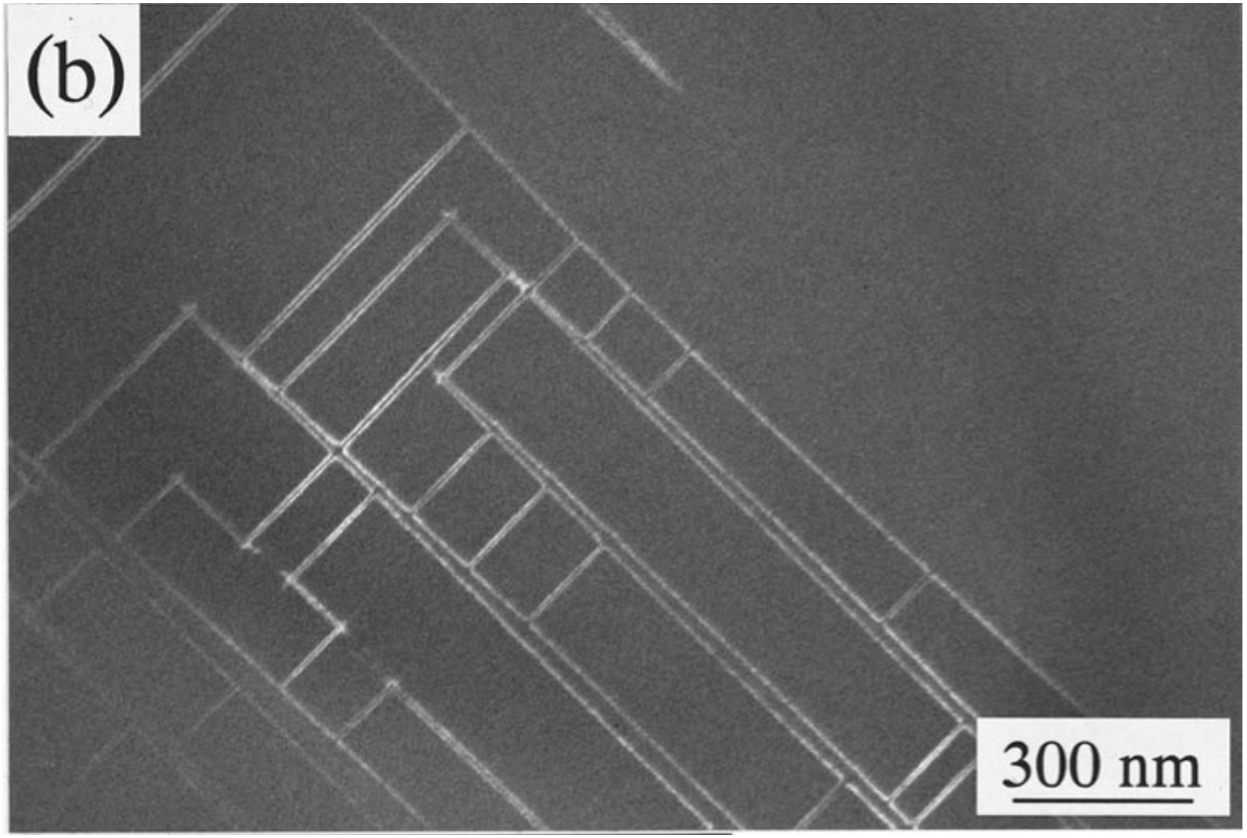

Domain model of LBCO Speckle Persistence

Pinning of the Ordered Charge Density Wave Phase in the Cuprates, X. M. Chen, Y. Cao, C. Mazzoli, V. Thampy, A. M. Barbour, W. Hu, M. Lu, T. Assefa, H. Miao, G. Fabbris, G. D. Gu, J. M. Tranquada, M. P. M. Dean, S. B. Wilkins, and I. K. Robinson, submitted (2018)

Domain model of LBCO Speckle Persistence

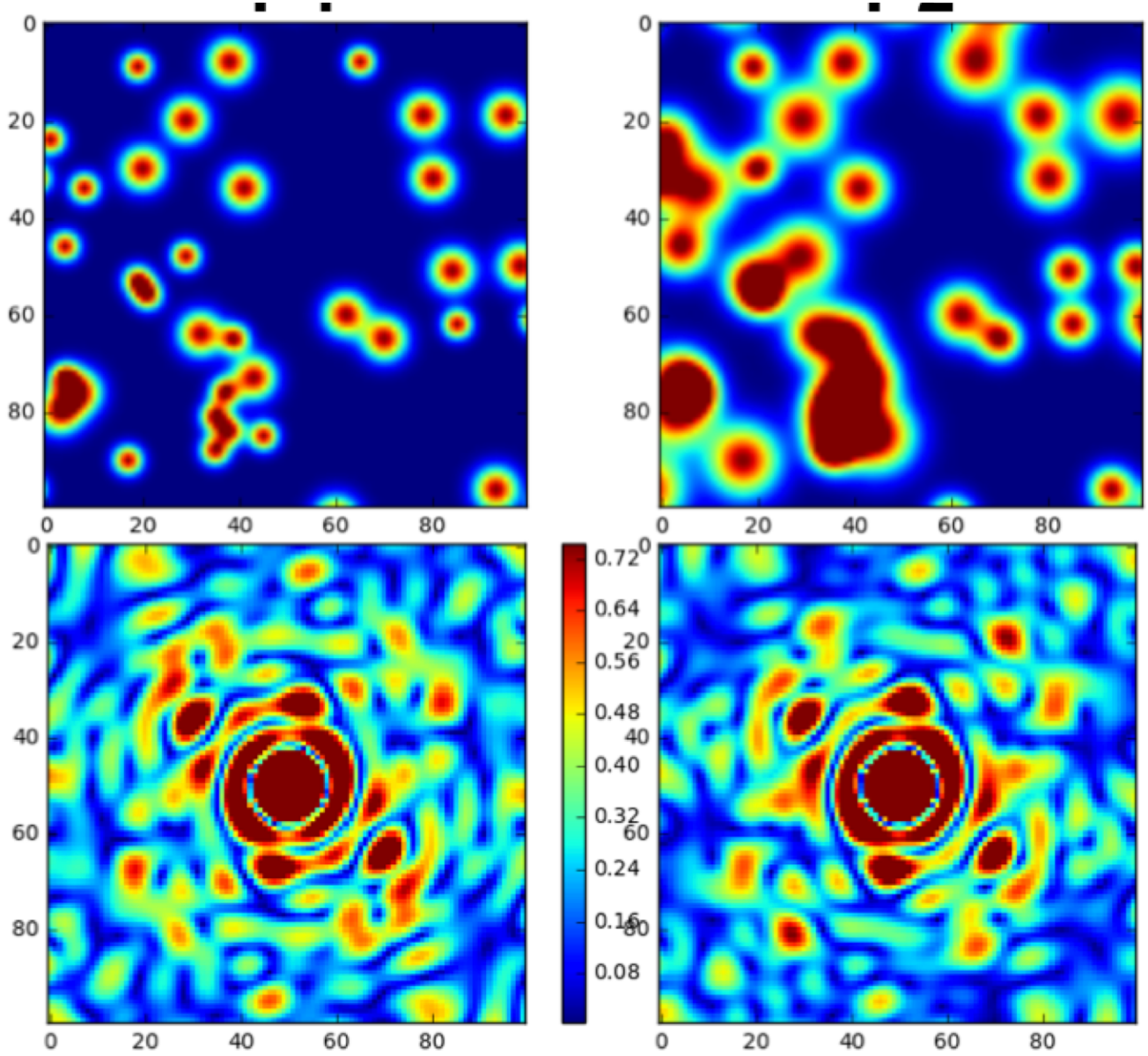

Tools to Image LBCO Domain Walls

- 012 peak forbidden in HTT, allowed in LTO phase
- Need well-formed micron-sized crystals for BCDI
- Need ultra-stable cryostat on a BCDI beamline
- Preliminary tests by grinding large crystals

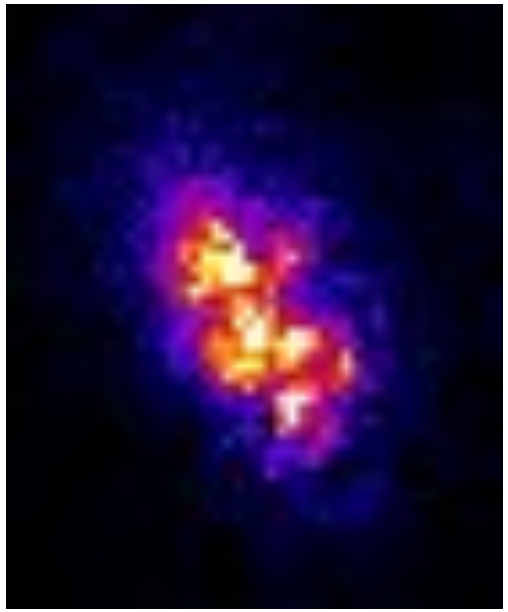

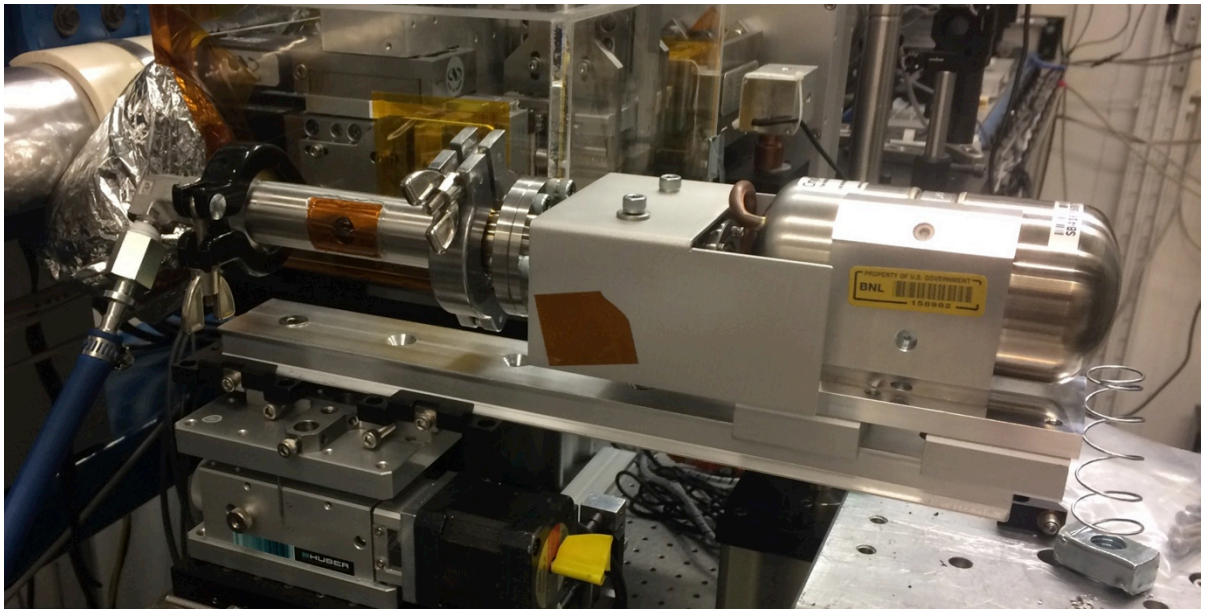

Speckle from LBCO Domain Walls

- Heating-Cooling cycles on LTO Bragg peak
- Change of speckle tells us the domain wall configuration has moved

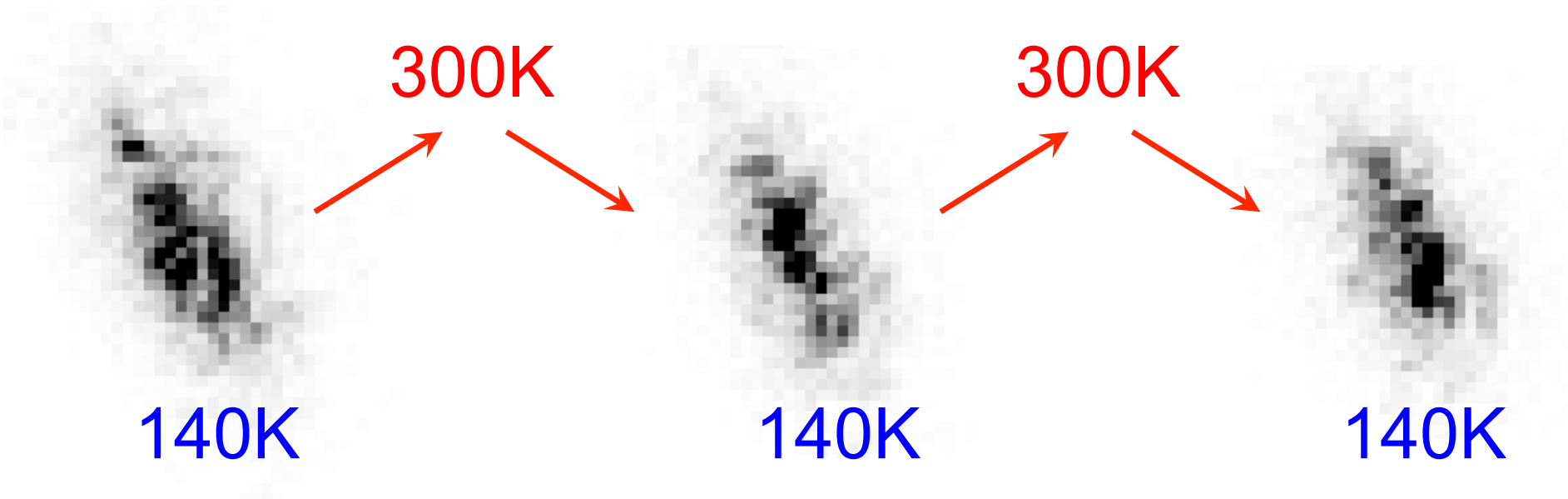

Preliminary BCDI image of LBCO stripes

CSX beamline at NSLS-II, Cu L_3 931eV (0.24,0,1.5) through pinhole array

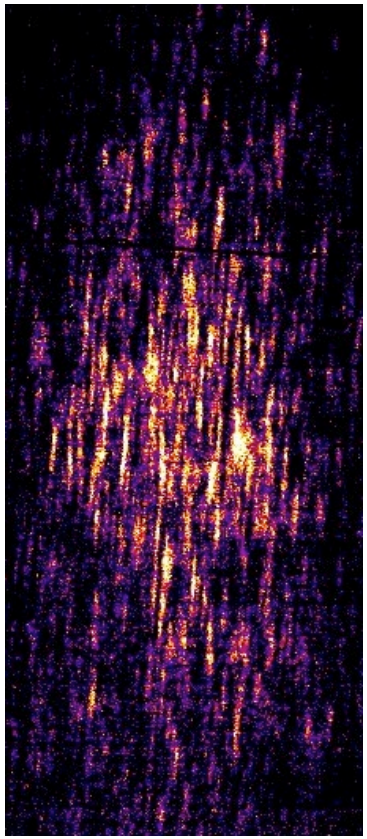

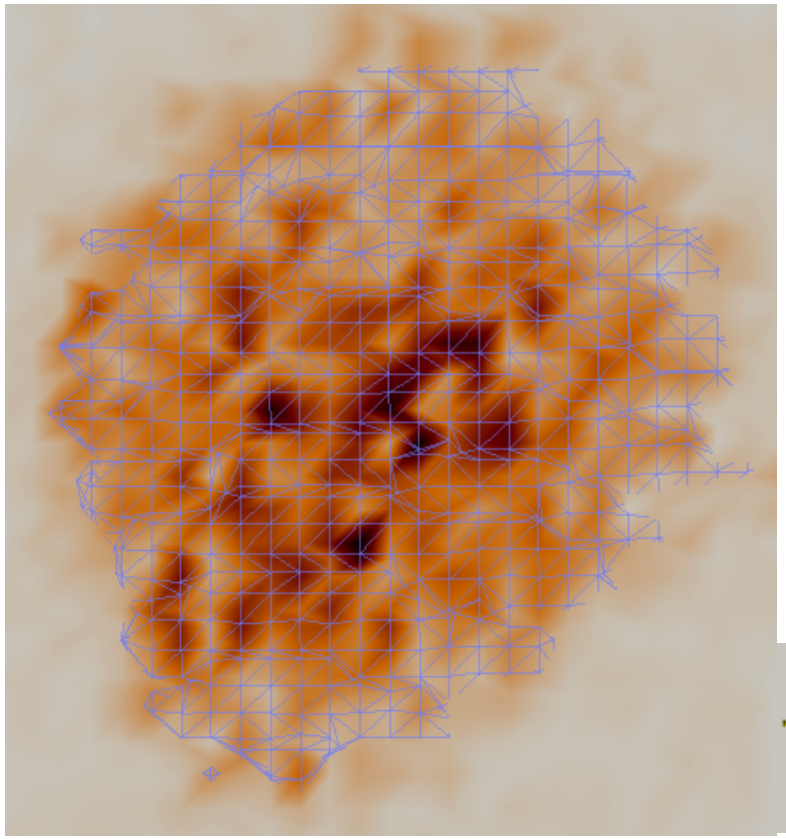

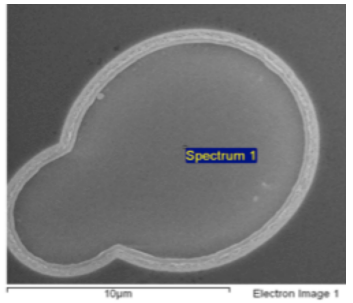

6.3 x 5.7 micron shrinkwrap support overlaid

Focused Ion Beam (FIB)

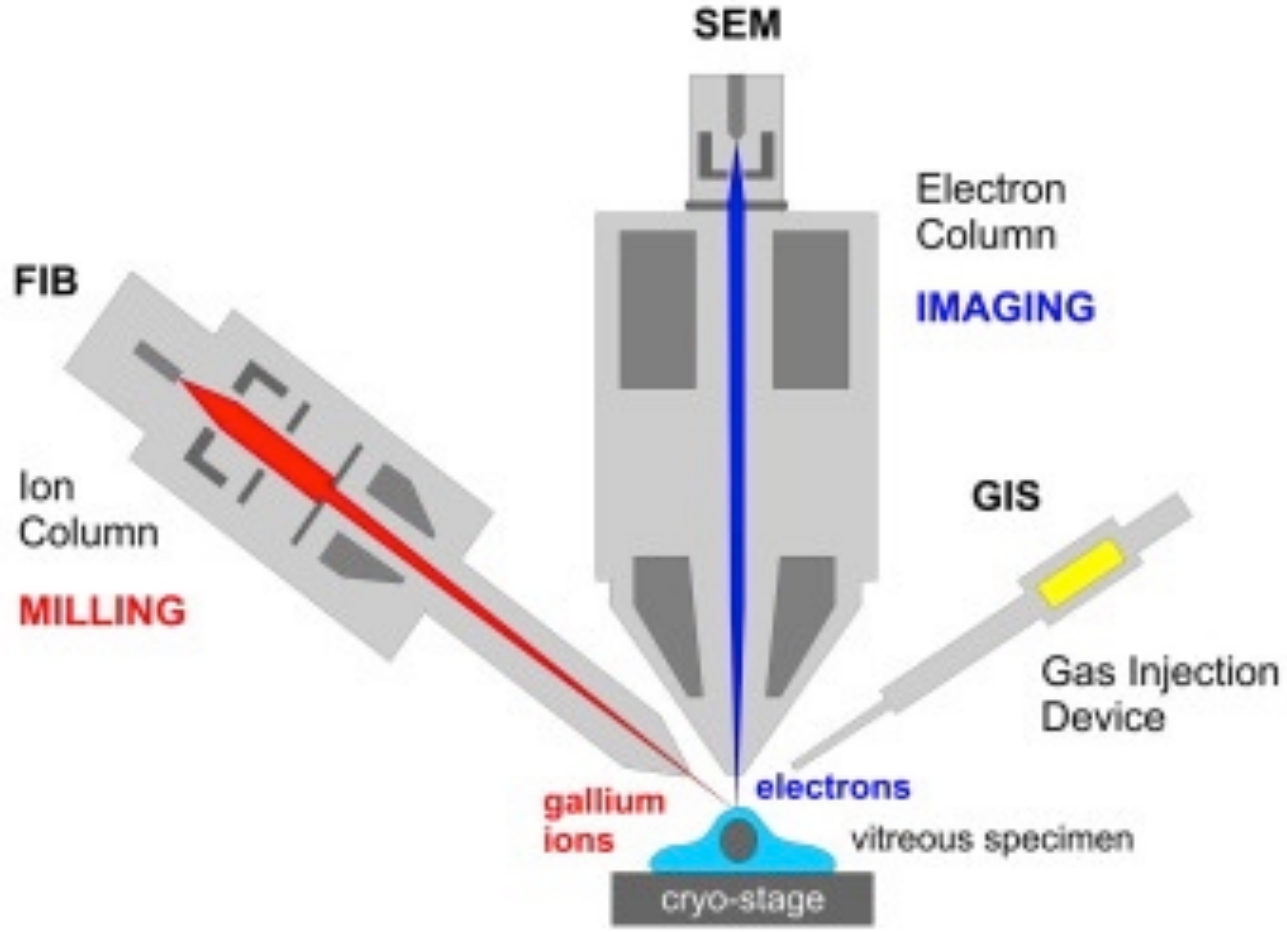

Unimplanted Gold Nanocrystals

Felix Hofmann, Oxford University 34-ID-C

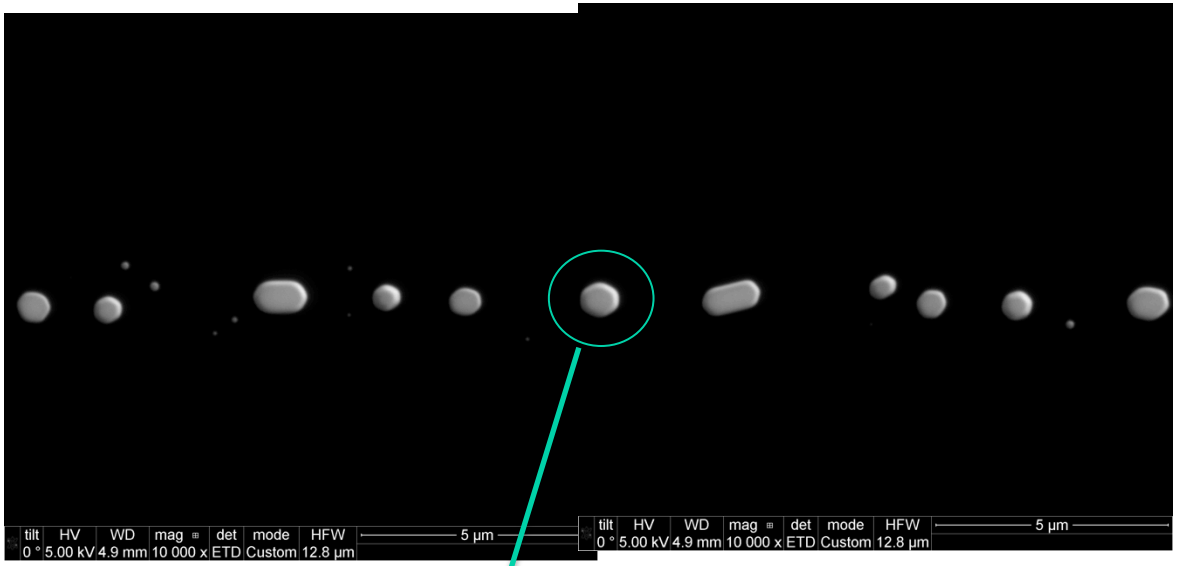

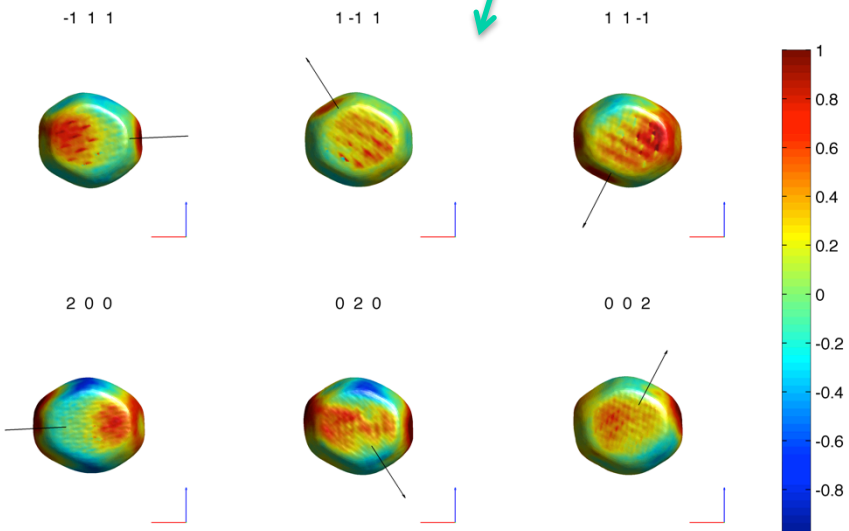

- measured 6 reflections at 9 keV. all phased fine.
- corrected for refraction-induced phase.
- worked out displacement field and hence strains

phases from different reflections

Shape comparison: BCDI and SEM

F. Hofmann et at Nature Scientific Reports 7 45993 (2017)

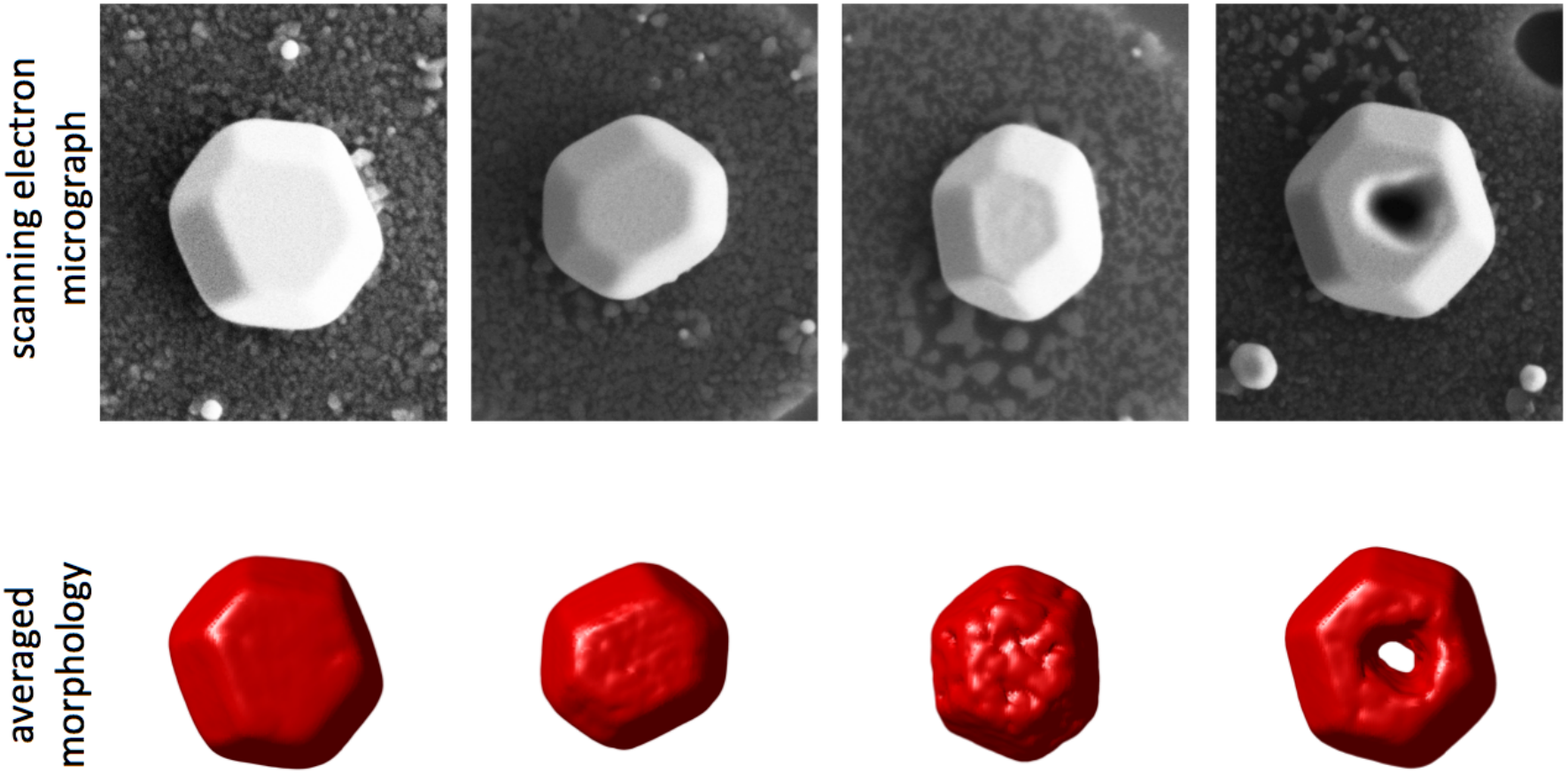

Starting crystal (yz plane)

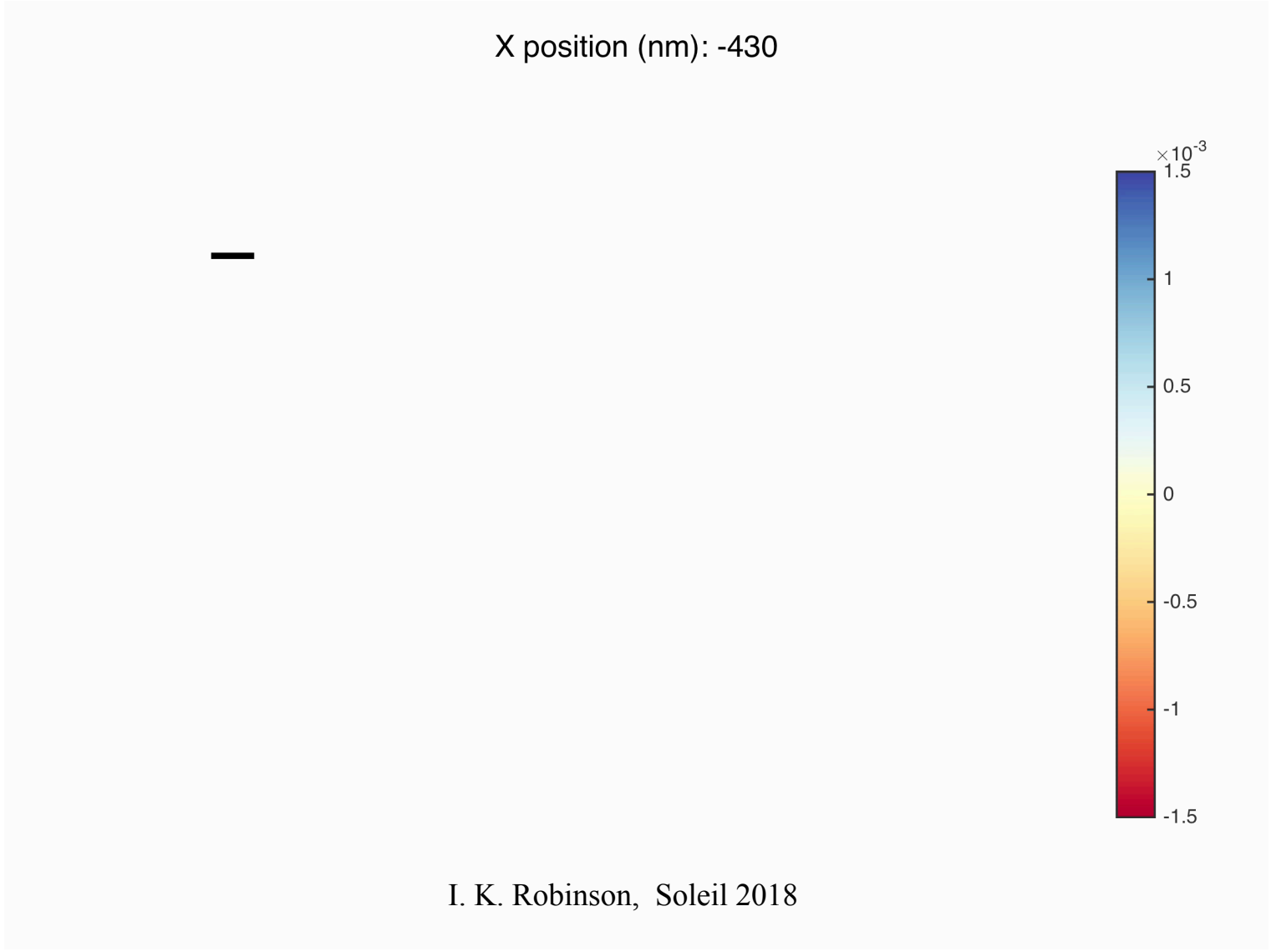

After irradiation (yz plane)

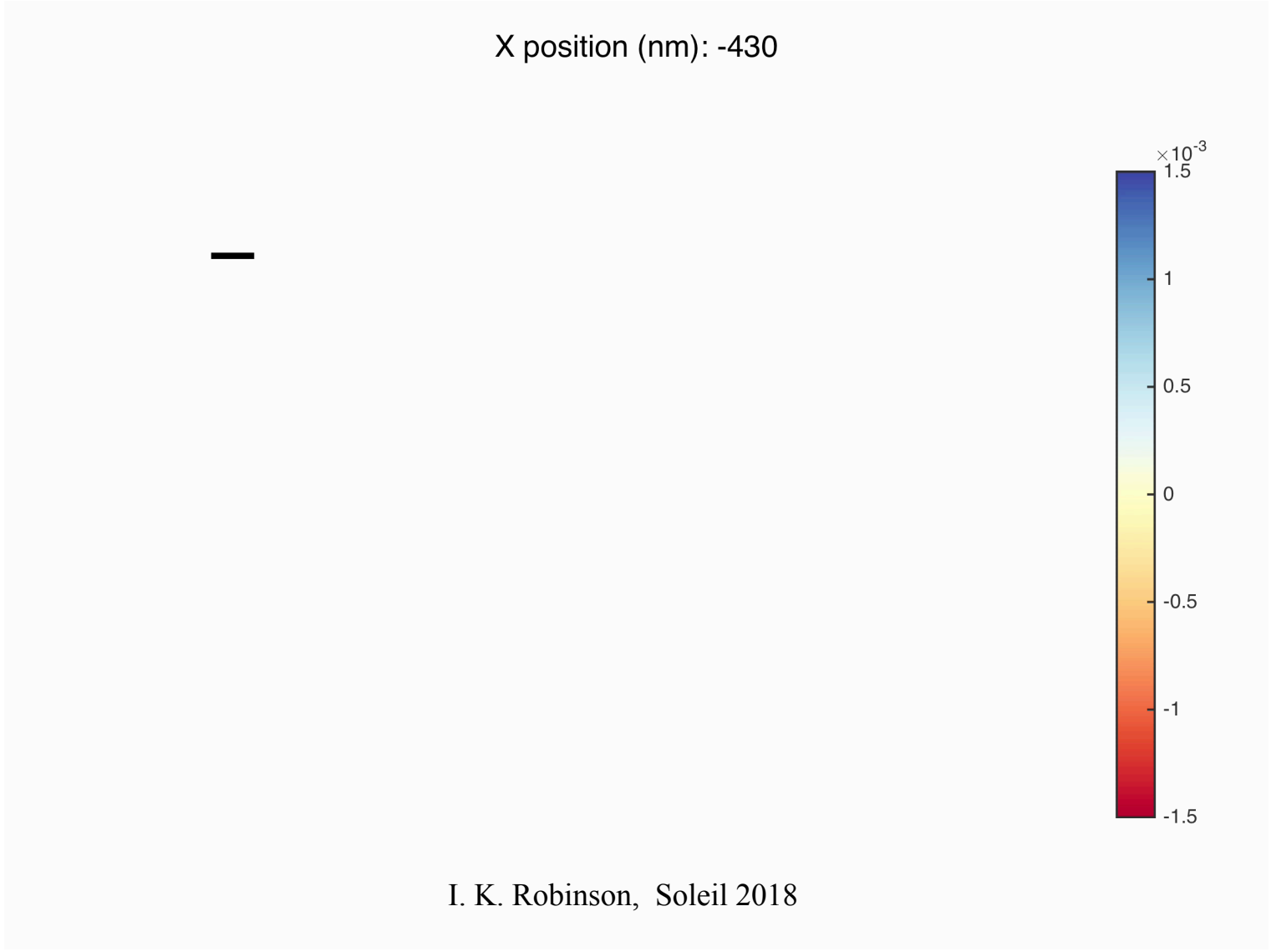

Dislocations

F. Hofmann et at Nature Scientific Reports 7 45993 (2017)

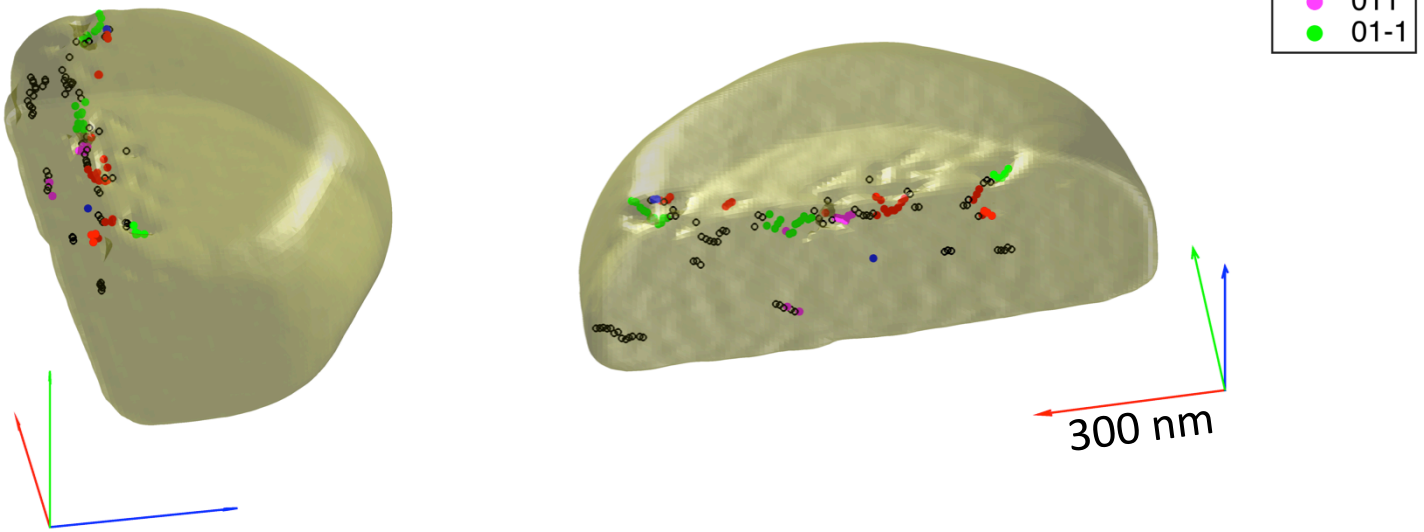

Amplitudes and phases of different reflections show jumps and pipes of reduced intensity consistent with dislocations. Dislocations identified in the crystal are shown above. They are colour coded according to their burgers vector direction, determined using Q.b contrast. Dislocations for which the burgers vector direction could not be identified are shown in black.

- dislocations are mostly formed at top edge of crystal where FIB beam has normal incidence component. These can form larger loops.
- some defects can also be seen on the milled face, although these are small.

Permalloy Magnetic Hysteresis
Permalloy $Ni_{0.8}Fe_{0.2}$

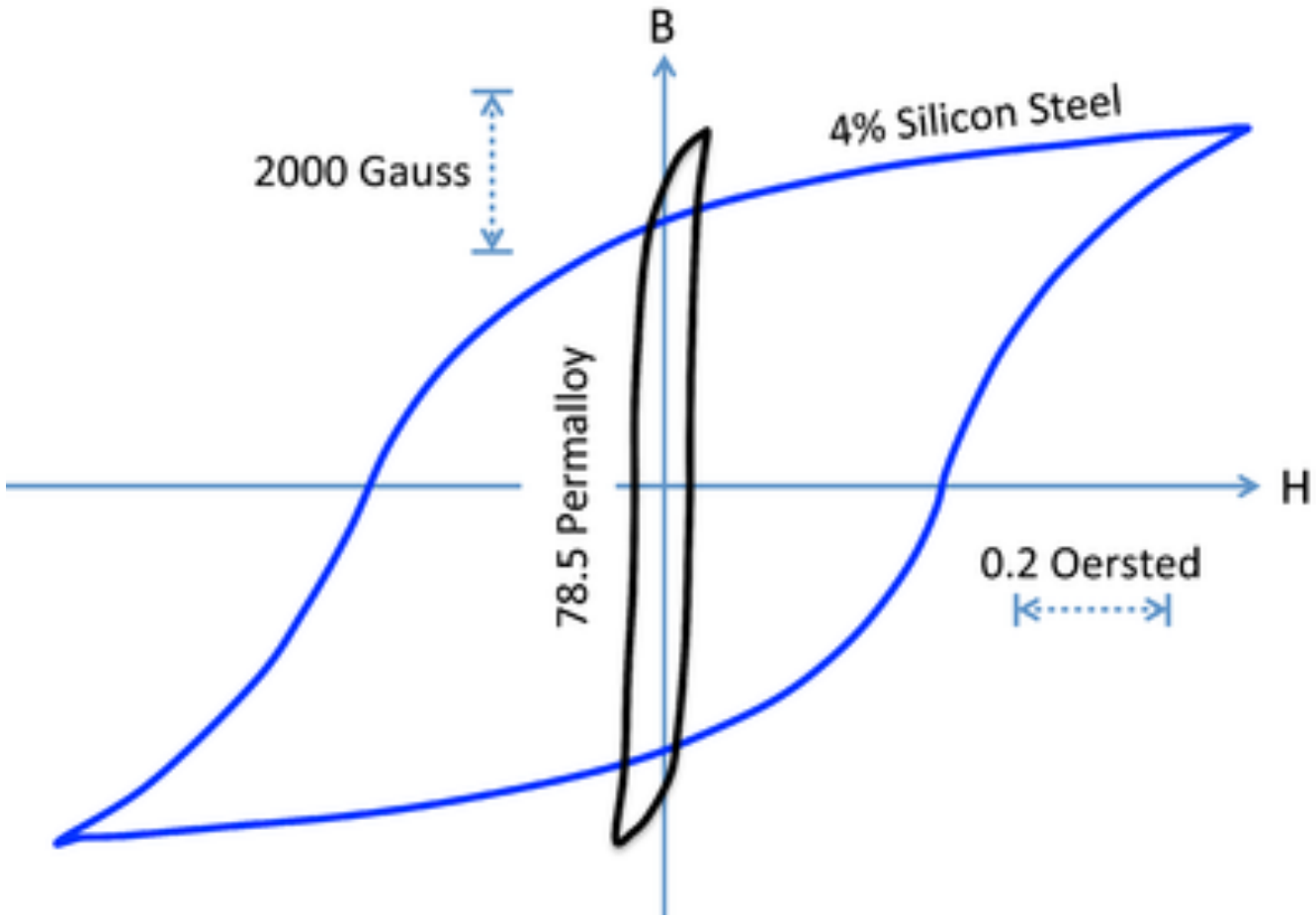

Artificial Spin Ice

Xiaoqian Chen, LBL, Todd Hastings, U. Kentucky

Permalloy $Ni_{0.8}Fe_{0.2}$

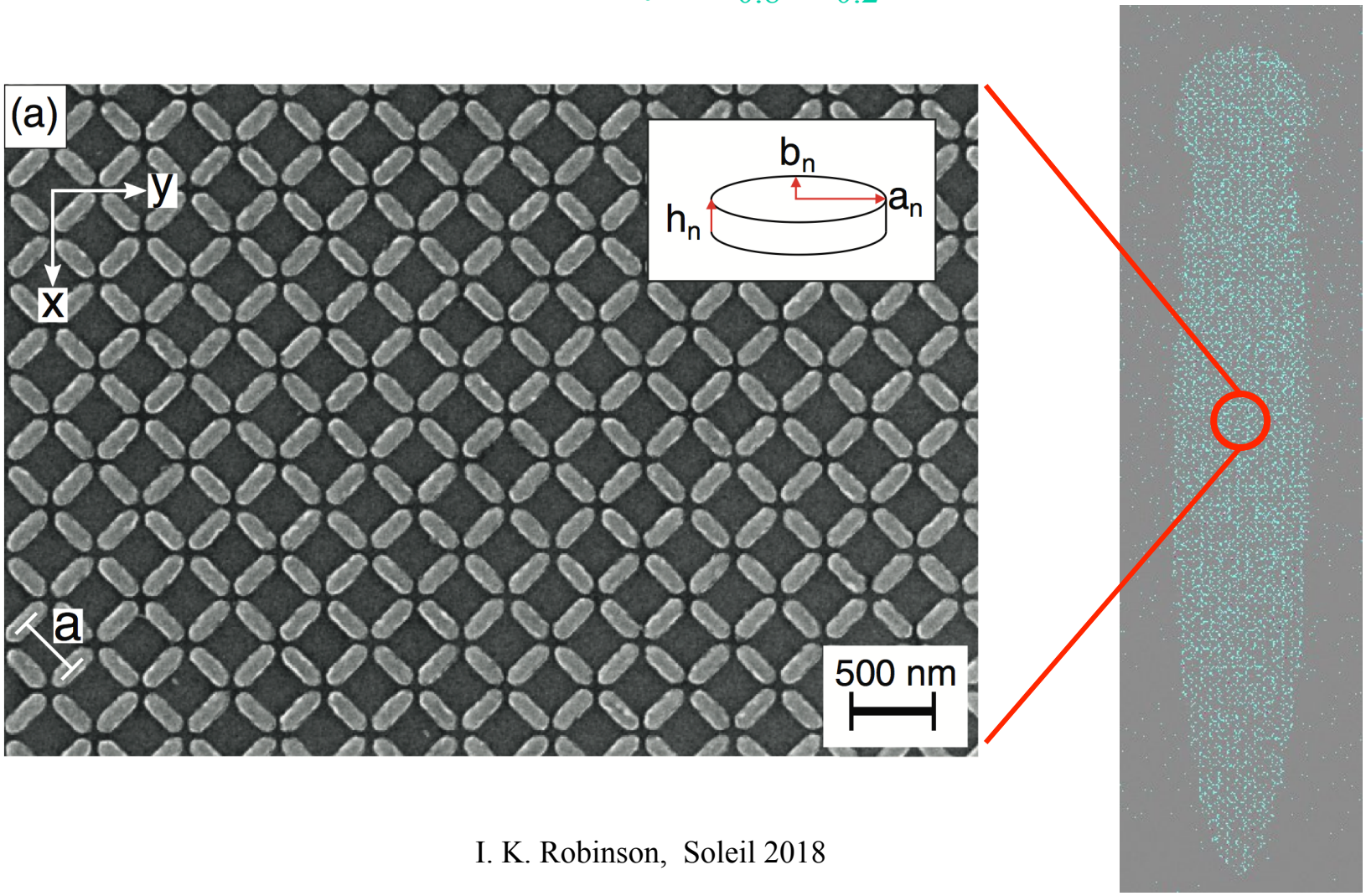

Artificial Spin Ice

Xiaoqian Chen, LBL, Todd Hastings, UKy, NSLS-II, CSX-1

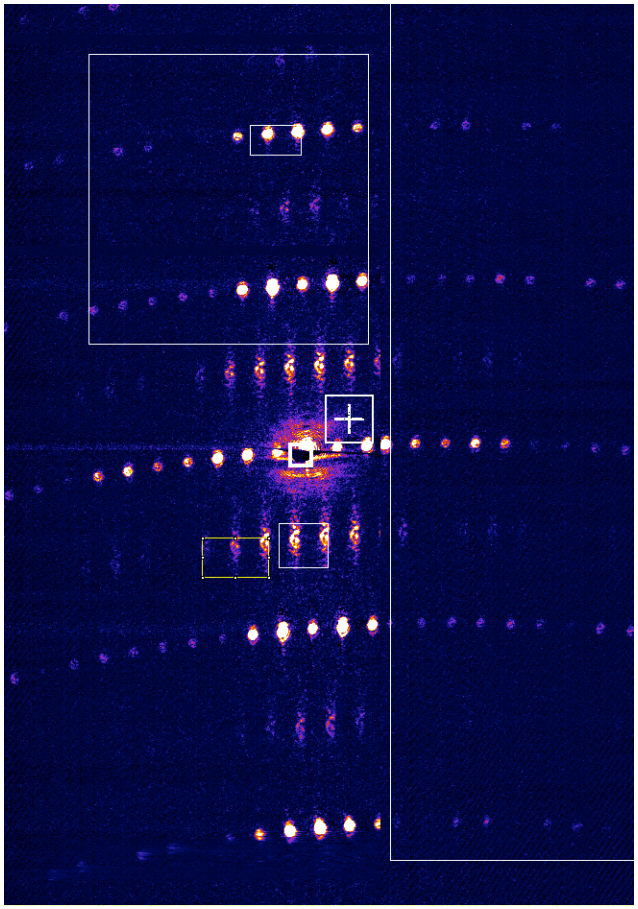

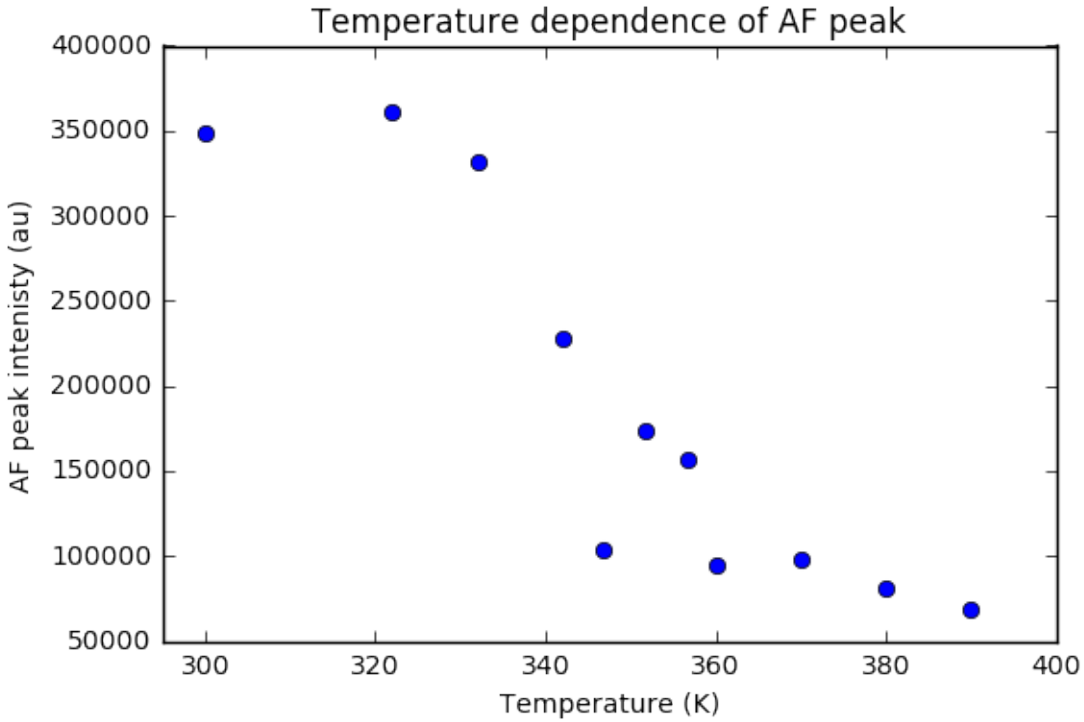

Magnetic scattering
On resonance at Fe-L_3 720eV

Artificial Spin Ice Reconstruction

Xiaoqian Chen, LBL, Todd Hastings, UKy, NSLS-II, CSX-1

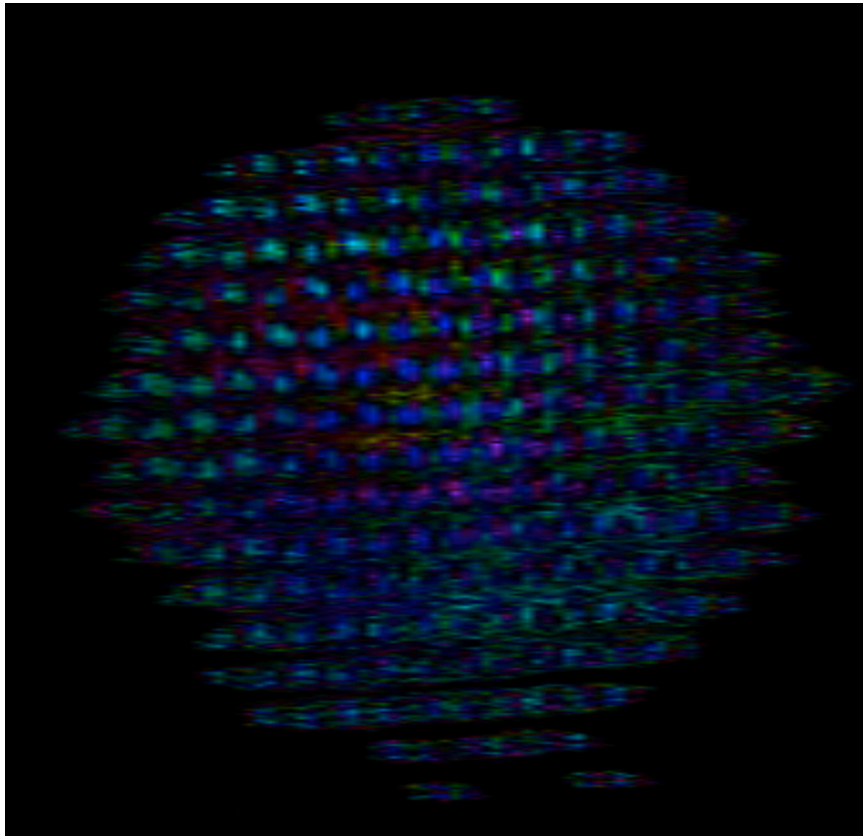

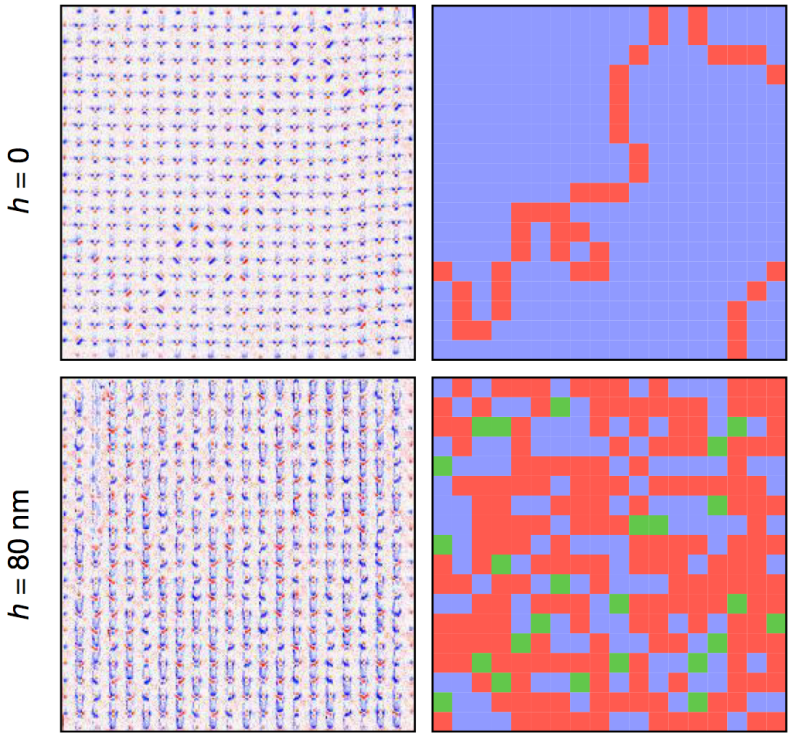

Magnetic Force Microscopy
Perrin et al Nature 540 410 (2016)

Bragg Coherent X-ray Diffraction

- Nanocrystal structures
- Bragg Coherent X-ray diffraction
- Domain Structures in Oxides
- $La_{2-x}Ba_xCuO_4$ HiTc Superconductor
- Focused Ion Beam (FIB) damage
- Artificial Spin Ice

The deadline to submit your abstracts for oral or poster presentations has been extended to ***Sunday, April 1st.***

Coherence 2018 is a conference that is dedicated to the use of x-ray, electron, and optical coherence for phase retrieval and coherent scattering, imaging matter, probing structures and dynamics.

Conference Dates: June 24-28, 2018

Conference Venue: Danford's Inn in Port Jefferson, NY

Registration: Early bird ends May 25 / Final registration closes on June 15.